Journal of Water Process Engineering 53 (2023) 103679

Contents lists available at ScienceDirect

Journal of Water Process Engineering

journal homepage: www.elsevier.com/locate/jwpe

Recent advances on humic acid removal from wastewater using adsorption process

Tamara Alomar [a], Hazim Qiblawey [a,*], Fares Almomani [a], Riyadh I. Al-Raoush [b], Dong Suk Han [c], Nasir M. Ahmad [d]

[a] Department of Chemical Engineering, College of Engineering, Qatar University, P.O. Box 2713, Doha, Qatar
[b] Department of Civil and Architectural Engineering, College of Engineering, Qatar University, P.O. Box 2713, Doha, Qatar
[c] Center for Advanced Materials & Department of Chemical Engineering, Qatar University, P.O. Box 2713, Doha, Qatar
[d] Polymer Research Lab, School of Chemical and Materials Engineering (SCME), National University of Sciences and Technology (NUST), H-12 Sector, Islamabad 44000, Pakistan

ARTICLE INFO

Keywords:
Humic acid
Wastewater treatment
Adsorption
Isotherm
Kinetic model
Regeneration

ABSTRACT

Humic acid (HA) is a component of natural organic matter (NOM) with a high molecular weight and high complexity. The presence of humic acid in water raises serious concerns due to its toxicity and ability to form carcinogenic trihalomethanes. Adsorption was shown to be an effective method for the removal of humic acid from various wastewater sources. Many adsorbents were feasible and effective for removing HA from wastewater, including carbon-based and activated carbons, clay-based adsorbents, zeolites, iron-based/magnetic adsorbents, functionalized adsorbents, and natural adsorbents. The removal of humic acid from water using different types of adsorbents was presented and reviewed and the effect of changing operational parameters such as pH, adsorbent dosage, contact time, initial HA concentration, temperature, and ionic strength on humic acid adsorption performance was evaluated. According to the review, the nano-MgO adsorbent performed the best in humic acid removal capacity, while MAER-3 resin performed the most regeneration cycles. Nano-MgO was the most promising adsorbent in capacity and regeneration capabilities, with an adsorption capacity of 1260 mg/g and ten regeneration cycles. Future research should focus on continuous adsorption processes in order to scale-up and use on an industrial level, as well as using actual wastewater rather than synthesized wastewater for adsorption experiments, as well as cost analysis to determine the feasibility of scaling up on an industrial level.

1. Introduction

Water scarcity is a growing global challenge caused by a combination of factors such as population growth, climate change, and unsustainable water use practices. With the rise in the Earth's population and the increasing demand for the depletion of freshwater sources, various strategies are put in place to improve the efficiency of water have been implemented. Wastewater treatment and reuse have been effective strategies, especially if the treated water can be reused. For countries that depend heavily on freshwater sources, the water quality must not be compromised, especially with natural organic matter (NOM) that is formed from the decay of plant and animal matter and include a range of compounds including humic and fulvic acids, amino acids, proteins, carbohydrates, and lipids.

Humic acid (HA) is a substance formed by decomposing organic matter, such as plants and animals, via biological and chemical processes. Humic acid is an organic substance with a very high molecular weight and is usually very stable and can be classified as recalcitrant and non-biodegradable [1]. It is a complex compound and does not have a definite shape or formula but rather a very complicated structure. Humic acid is abundant in natural waters as total dissolved organic carbon (DOC) [2] and since HA is an organic compound, it could also be quantified using COD which is able to indicate organic pollution in various types of wastewater [3]. HA is prominent in natural surface water such as lakes and rivers and has a concentration varying from 0.1 to 20 ppm [4] and even more than seawater since the freshwater environment possesses a greater fraction of organic material. Furthermore, humic substances can be found in municipal wastewater with a concentration varying from 118 to 228 mg/g, and approximately 42 % of these humic substances represent HA [5]. The presence of HA structures

* Corresponding author.
E-mail address: hazim@qu.edu.qa (H. Qiblawey).

https://doi.org/10.1016/j.jwpe.2023.103679
Received 6 January 2023; Received in revised form 6 March 2023; Accepted 21 March 2023
Available online 30 March 2023

in water results in undesirable properties especially in domestic or drinking water supply, such as odor, color, and taste [6]. In addition to their contribution to the formation of disinfection byproducts in the presence of trihalomethanes [7] that compromise consumers' health. Therefore, the need for the removal of HA becomes a necessary procedure in wastewater treatment.

There are variable methods for the removal of HA from wastewater such as filtration, flocculation, oxidation and biological processes are traditionally used [1]. New technologies are emerging continuously, and different removal strategies are being investigated. However, the most prominent and most researched ways of HA removal include adsorption [8], membrane filtration [9], flocculation and coagulation [10], advanced oxidation processes (AOP) [11], biological treatment [12] and emerging integrated/combined processes [13]. In this review, the focus will be on the adsorptive removal of HA from wastewater. In comparison with other wastewater treatment processes, adsorption presents as a highly effective method for wastewater treatment in terms of its simplicity, low cost and variety of target pollutants that can be removed.

A comprehensive literature review was done using three main search engines: 'Scopus', 'Google Scholar' and 'Web of Science'. The time frame of interest was from the year 2011 to 2022, this is to allow for the investigation of the most recent technologies in the literature in the past decade. The main search criteria were using the keywords "Humic Acid" AND "Water Treatment" AND "Review" to search for relevant review papers that aided in having the initial scope of the study. This was followed by another search criteria using the keywords "Humic Acid Removal" AND "Adsorption" when searching for adsorption processes. This yielded 89 articles which are demonstrated in this paper, 45 of them are related to the adsorbents mentioned in this paper. The different papers that were found through the literature search of humic acid adsorption per year are shown in Fig. 1, where the data was extracted through WoS database. It is also obvious that the publications relating to humic acid adsorption are relatively more in the past couple of years due to the topic being of high importance and that is why the light was shed on this topic specifically. It is worth noting that the HA field of research is tremendously large, and it was difficult to select the most related papers to the adsorption of humic acid exclusively.

This review classifies the adsorbents into seven main categories: Activated carbon and carbon-based adsorbents, clay-based adsorbents, zeolite/resins, iron-based/magnetically reclaimed adsorbents, polyaniline-based, functionalized and unrefined (natural) adsorbents. The biggest challenge faced when establishing this review was the classification of the adsorbents. However, the methodology that was followed was based on the resources found; this is explained further in Section 3.

Numerous review articles have been published on the topic, specifically in combination with fulvic acid removal or simultaneous removal of humic acid and metals for example. Several review articles exist in the literature that highlight the removal of HA from wastewater through adsorption processes. A review conducted by Aminul Islam et al. [14] studied the effect of the presence of HA and fulvic acid (FA) on the adsorptive removal of other pollutants such as heavy metals in water. The removal of both HA and FA using nanotechnology was investigated by Tang et al. [15], in addition to the impact of HA and FA on the removal of heavy metal ions existing in wastewater such as lead, cadmium, copper, etc. The review carried out by Bhatangar and Sillanpaa [16] overviewed the adsorptive removal of natural organic material (NOM) in general, and the different adsorbents that can be utilized for NOM adsorption from wastewater. Other review articles have highlighted adsorbents such as biochar [3] for the remediation of potable water. Several pollutants were able to be removed using biochar including pesticides, dyes, and most importantly humic acid (60 mg/g). These studies focused on the adsorption of both HA and FA, or the effect of their presence on the removal of other compounds such as heavy metals and not on the adsorbents available for solely removing HA from wastewater. In this review, the main focus will be on the adsorptive removal of HA alone from wastewater, the different adsorbents that could be utilized, and the factors affecting HA removal.

The main objective of this paper is to present a comprehensive scope of the current state of the literature on the adsorptive removal of HA alone and investigate the different adsorbents that could be used for the removal of HA from wastewater, as well as the different operational parameters that affect the adsorption process. The properties and brief insight into the humic acid structure, its properties, sources, and toxicity would be presented. Moreover, the significance of the kinetic and isotherm study parameters as well as the regeneration potential are to be discussed. The suggestion of the best adsorbent for HA removal was based on two main criteria: adsorption capacity and reusability of the adsorbent. Moreover, gaps in the literature were analyzed to predict the future trends of humic acid removal in water research.

2. Humic acid properties

2.1. Sources of humic acid in water

Humic acid is usually found naturally in the soil and is formed as a result of the chemical or biological degradation of living matter (animals or plants), and therefore exists in groundwater, peats, freshwater and even in oceans but varies in concentrations. Natural waters contain <10-15 mg/L of HA as reported in the literature [17]. Humic acid can be

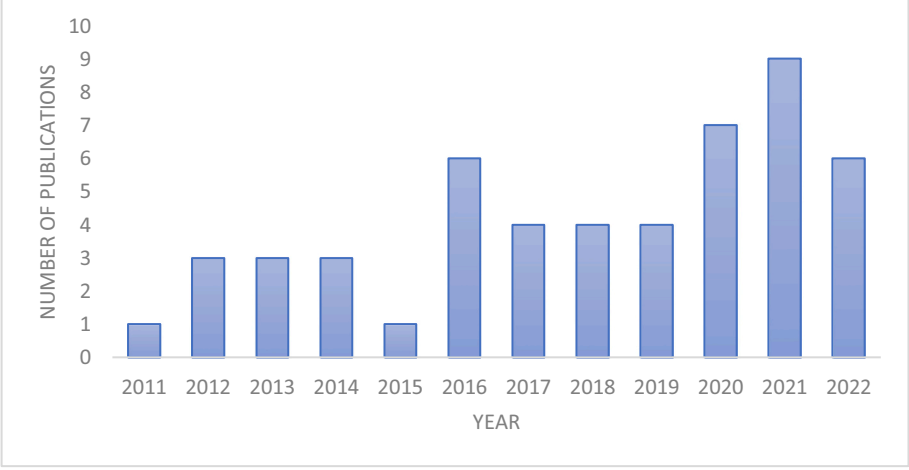

Fig. 1. Publications per year for humic acid adsorbents found in literature and reviewed in this paper.

extracted from crop plants as well as animal waste [18] and is usually used as a buffer for the soil and enhances the environment of the soil so that the conditions are ideal for nutrient absorption by the plants.

Fig. 2 shows an illustration of the formation of HA from organic matter in natural systems. When the organic matter decomposes entirely due to chemical and biological degradation (which is facilitated by moisture and bacteria), once the material cannot decompose any further, it is called humus. This humus/humic substance would be split into three main substances: humin, humic acid, and fulvic acid. Humin is the insoluble fraction, it would not dissolve in both acidic and aqueous solutions, while humic acid is the soluble fraction in alkaline solution but not acidic, and fulvic acid is soluble in acidic solutions. There are four primary sources of HA, but the main mechanism of formation includes complex polyphenols reacting or complexing with amino acids. Lignin or lignin-like materials can act as the polyphenol source, or the lignin can react with other aromatic compounds producing polyphenols. Polyphenols can also originate from cellulose, starch and other sugars that are consumed by microorganisms, and leaf polyphenols can also react with amino acids existing in leaves and soils [19]. This acknowledges the source of humic acid formation to be plant and animal residues in the soil.

Humic acid can be found in various types of wastewaters, including municipal/domestic, industrial, and agricultural wastewater. The presence and concentration of humic acid in wastewater depend on several factors, such as the source and characteristics of the wastewater, the treatment processes used, and the presence of other contaminants. In industrial wastewater, humic acid can be present as a result of various industrial processes and can vary with the type of industry. Humic acid has been found to be a product of the cellulose and paper-processing industry [20], oil mills wastewater treatment through composting techniques [21], the food processing industry [22], and tannery wastewater [23]. It was also found that the industrial wastewater that was biologically treated contained a significant brownish color [24], this suggests the presence of humic and fulvic acids and poses a significant issue in terms of toxicity and aesthetics. In agricultural wastewater, humic acid can be present as a result of the decay of plant material, irrigation effluent and livestock waste. Livestock wastewater treated via reverse osmosis process resulted in the formation of concentrate containing humic acid [25]. Moreover, landfill leachate contains high amounts of humic substances such as HA, FA and humic substances [26]. Municipal/domestic wastewater undergoes treatment using secondary biological treatment processes such as the activated sludge process. The waste activated sludge contains a high amount of humic acid, which can leach back into the wastewater and disrupts the treatment process as well as the quality of the effluent water [27–29]. This reinforces the need for tertiary wastewater treatment processes for the removal of HA or other humic-like substances. Overall, humic acid can be found in various types of wastewaters, and its presence can impact the efficiency of wastewater treatment processes. Therefore, understanding the composition and properties of humic acid in wastewater is crucial for the effective treatment and management of wastewater resources.

2.2. Structure and composition of humic acid

The structure of HA is quite complex and uncertain, and due to many factors affecting the formation of humic acid, there are no two identical structures [18]. However, many structures were proposed by scientists due to continuous, dynamic changes in the HA structure that continuously undergoes humidification [30]. It can be agreed upon that the HA structure is defined as a polymer with an aromatic core and aliphatic chains with multiple functional groups such as amines, alcohols, ether, phenyl, aldehyde, ketone, carboxylic, ester, amide and quinones [30,31]. Generally, aliphicity in the HA structures is much greater than total aromaticity [18] where it was reported that the HA structure is 35 % aromatic, while the balance is aliphatic [32]. FTIR results of HA sourced from the soil in the Indian city of Karnataka are shown in Fig. 3, where 7 main peaks were identified [33]. The first peak is a strong but broad peak at 3246 cm^{-1} that demonstrates the presence of H bond to OH, this suggests the presence of alcohol structures. The second peak at 1721 cm^{-1} correlates to a C═O bond that could be attributed to the presence of ketones, aldehydes and esters. The third peak at 1634 cm^{-1} signifies the presence of alkenes (C=C) as well as the C═O bond of carboxyl and quinone structures. The fourth peak occurring at approximately 1450 cm^{-1} represents the aliphatic C—H which indicates alkane structures and methyl groups, this is expected due to the high percentage of aliphicity discussed earlier. The fifth peak at 1112 cm^{-1} represents

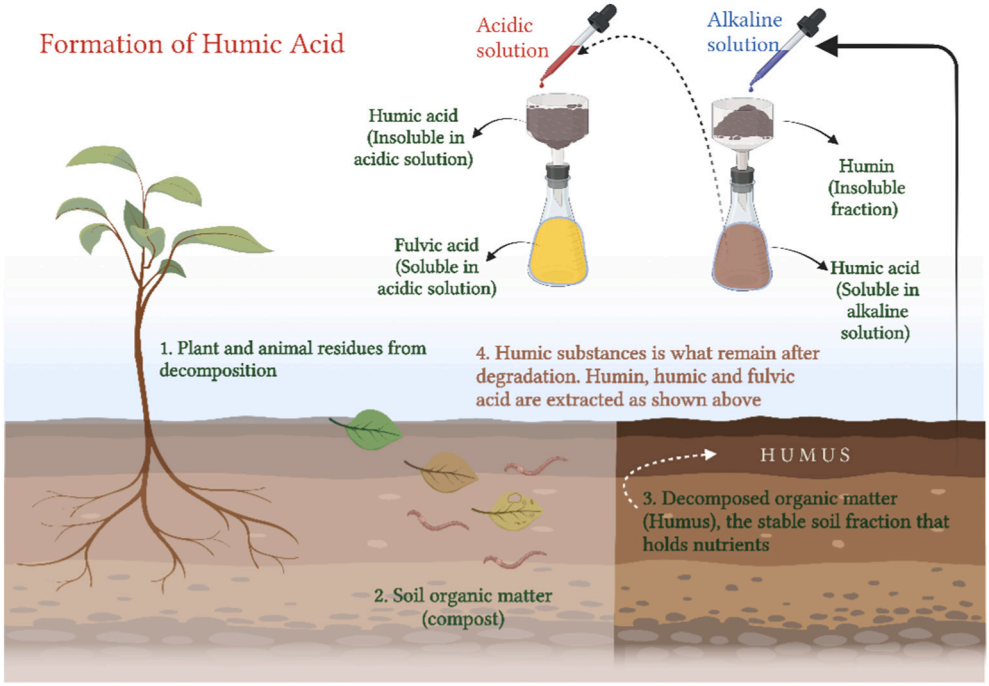

Fig. 2. The humic acid formation process.

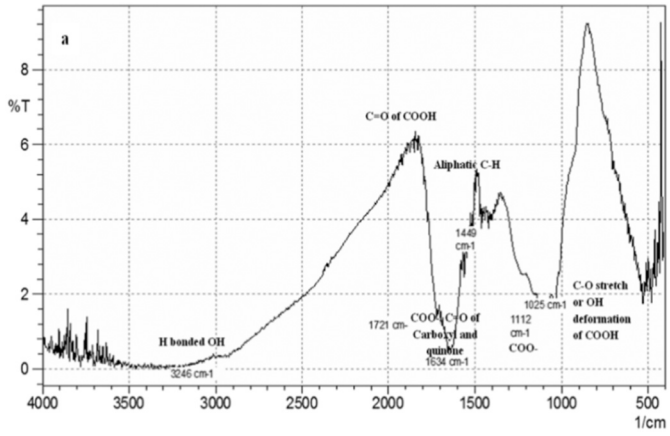

Fig. 3. FTIR of soil humic acid sample [33] (copyright under the terms of CC BY-NC-SA 3.0).

the COO^{-}, and the sixth peak at 1025 cm^{-1} represents the C—N stretching of the amine group. The last peak occurs at approximately 850 cm-1, representing the C═C bending or the bonding of C—H [34]. Peaks in the functional groups such as COOH and quinone groups are consistent with information discussed in theory for the FTIR spectrum [35].

There are multiple structures of HA proposed in the literature; some of these include Dragunov, Steelink, Shukten & Shnitzer, Stevenson, and Flaig's structures of humic acid and these are illustrated using Fig. 4a–e. The structures would contain all or most of the functional groups mentioned above when discussing FTIR analyses. The most complex structure is the one proposed by Shnitzer and Schulten [36], it can be observed in Fig. 4c that hydroxyl and carboxyl groups are abundant on both aromatic and aliphatic side chains and rings.

The chemical composition of HA varies with the geographical origin, age, climate and biological conditions [40]. In addition to the chemical composition variations, the elemental composition also varies slightly depending on the source of the humic acid. On average, the HA structure would predominantly be composed of carbon, hydrogen, nitrogen, and some sulfur compounds. In conjunction, the percentage of oxygen differentiates HA from fulvic acid (FA) structures, as FA has more oxygen content than HA [41]. Fig. 5 shows the elemental composition of HA obtained from 14 different sources, where it is evident that >50 % of the structure is carbonaceous followed by oxygen composing approximately 26 % of the structure [42].

2.3. Properties of humic acids

Although humic acid has no definitive structure due to the presence of different functional groups. Still, there is a trend to be found in the properties such as hydrophilicity, ion exchange capacity, surface charge, molecular weight, solubility, and acidity.

HA has a significant molecular weight, usually ranging from 500 to 250,000 Da [43]. Therefore we can refer to HA molecules as macromolecules due to their large molecular weight and complex structures. In addition to the large molecular structure, HA molecules have large surface areas ranging from 800 to 900 m^2/g [44] and can be used as adsorbents themselves [45], especially for heavy metals or metallic ions due to a "ligand-like" property.

HA molecules are considered weak polyelectrolytes and can exist as dissolved or in a dissociated form in water. The insoluble fraction interacts with the environment as an ion-exchanger by releasing protons (H^{+} ions) into the solution while the anions remain insoluble [31]. Furthermore, HA molecules were found to be soluble in neutral to alkaline conditions as they tend to precipitate in acidic media, and this is because as pH falls in the acidic region (pH < 2), the HA acid structure becomes spherical and precipitates [1,46]. This is an indication of the effect of pH on the performance of removal processes of HA from aqueous solutions or water.

HA is considered one of the most charged natural polyelectrolytes that can be attributed to the many functional groups that are available on the surface. It was reported to have 3-4 charging sites per 100 Da [47,48]. Moreover, the cation exchange capacity (CEC) is less for HA (485-870 mol/kg) than for fulvic acid [44], nevertheless, the presence of HA in soil enriches its fertility and the three vital nutrients can be supplied (potassium, calcium and sodium). HA generally exhibits a negative charge due to the carboxylic and phenolic functional groups that are

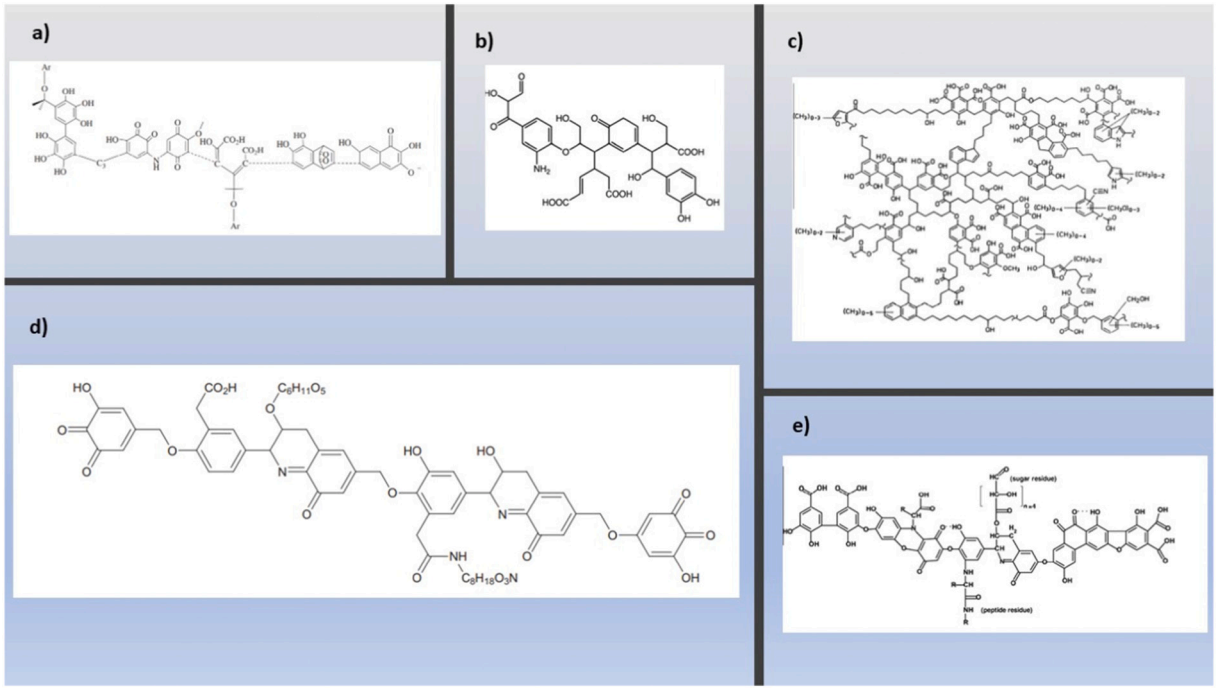

Fig. 4. Different structures of humic acid as proposed to by: a) Flaig [37], b) Steelink [38], c) Schulten and Schnitzer [36], d) Dragunov [18], and e) Stevenson [39].

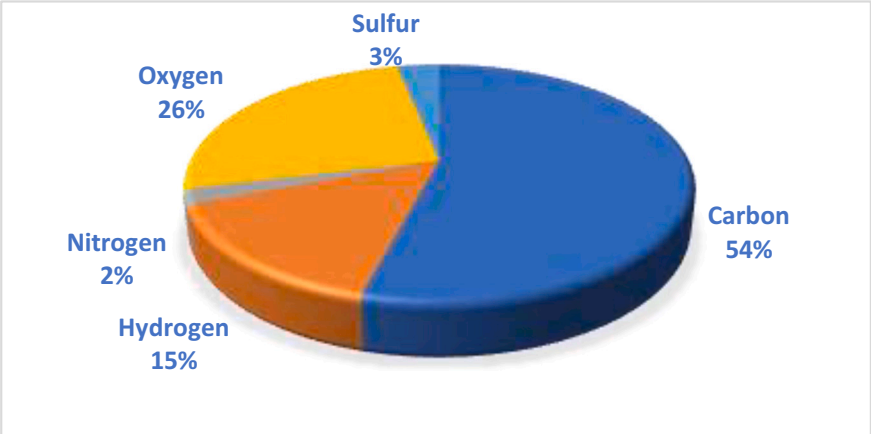

Fig. 5. Average elemental composition of 14 humic acid sources [42,129–131].

abundantly present on the structure's surface [49]. It was also observed that zeta potential is negative at pH above approximately 2, while it is positive at pH below 2. This is explained by the dissociation of H^+ ions or deprotonation of carboxylic and phenolic groups above this pH value [50] which means they usually exist in anionic form. Therefore, it is expected that the HA structure would always be anionic since maintaining a pH of 2 is uncommon, especially in the water treatment industry due to cost and safety issues at such low pH values.

HA molecules can exhibit detergent characteristics at low pHs (<2), where the functional groups get protonated (less repulsion) and form compact micelle-like structures with the hydrophobic part being enclosed within the structure and the hydrophilic part being towards the aqueous medium. With time, these micelle structures aggregate and eventually precipitate. These surfactant characteristics are beneficial for the cosmetic and pharmaceutical industries [31]. Another characteristic of HA is its chelation ability, or the formation of complex compounds when it combines with heavy metals and acts as a ligand, this is useful in many applications such as [31]; transportation of micronutrients to plants via soil and water, removal of heavy metals from water or soil, inhibition of free radical formation and reduction and stabilization of metal nanoparticles.

The shape of HA is affected by the pH of the surrounding environment, at low pH values, HA is a spherical coil while at high pH the shape of HA is linear due to the repulsion of the charges [51], and the particle size also increases with increasing electrolyte concentration [30]. The color of HA is influenced by the functional groups present, pH and redox potential. The color also increases (becomes darker) with increasing polymerization, molecular weight, and carbon content [30].

2.4. Toxicity of humic acids in water

Humic acid is classified as a stable but complex organic compound that is considered recalcitrant (non-biodegradable) [1]. HA in soil affects the soil properties by enhancing the soil's color, affecting the heating rate, improving air-water relations, porosity, viscosity and soil compaction, and having large water capacity. This is good for plants since HA can act as a source of nutrients for plants and protects plants from diseases [30]. Fig. 6 shows the effect of adding HA to the soil. Clearly, with the addition of HA (Liqhumus) the root structure is enhanced and therefore explains the enhanced soil properties and enhanced nutrient and water capacity.

However, HA is not environmentally degradable, and its accumulation causes problems related to the odor, taste and color of the water and therefore causes the spread through water distribution systems and could also act as a nutrient source for the microbes in these systems [16,52,53]. The spreading of these microorganisms can cause major health effects on humans since their presence makes the water

Fig. 6. Comparison of root structure using humic acid (right) and without humic acid (left) [132].

unhygienic and unsuitable for human consumption. Furthermore, HA could also contribute to membrane fouling even after the backwashing process and increases the cost of replacement of these membranes which is undesirable. Membrane fouling due to the presence of HA affects the performance of ultrafiltration membranes, and that is why some studies use HA for modeling the antifouling potential of membranes [54,55] in relation to other studies that utilize wastewater effluent [3].

HA in water can induce the production of disinfection by-products (DBPs) due to their interaction with chlorine and disinfectants, which can be harmful to humans. HA is classified by the International Agency for Research on Cancer (IARC) as a category 2A or 2B, which suggests that the presence of HA in water is probably or possibly carcinogenic for humans [8]. The presence of these DBPs can also induce other health effects such as central nervous system (CNS) problems, reproduction system defects, retardation in growth, anemia, and cytotoxic effects (which suggest damage to the cells) as well as genotoxic effects [7].

Other harmful effects of HAs on humans include teratogenic properties, which negatively affect the fetus development and mutagenic

effects, which suggest the mutation of cells in the human body [1]. Other studies have found that HA consumption contributes to Blackfoot's disease [56]. This suggests that the presence of HA in water should be regulated so that people's health is not compromised.

3. Adsorption for HA removal from wastewater

Adsorption is one of the most effective processes for removing pollutants from water. Adsorption is a mass transfer process involving the adsorbate's attachment to the pores on the adsorbent surface, as illustrated in Fig. 7. The mechanism of this attachment can vary depending on the type of adsorbent and the interaction between the adsorbent and adsorbate. The adsorption process could be carried out for the removal of HA using different types of adsorbents, most commonly: activated carbons (AC), clays, zeolites and many other classifications. The extent of adsorption depends highly on the adsorbent surface and how it interacts with the pollutant to be removed and the physical properties of both the adsorbent and adsorbate. The experimental conditions also play a vital role in this process, and this is discussed further in Section 5. Some advantages of adsorption compared to other removal processes is the economic nature of adsorption, ease of setup, high reusability achievement as well as high efficiency of the process which makes it desirable for wastewater treatment.

Although there were difficulties in clearly classifying the adsorbents as some of them could be classified under more than one subsection/category. For example, when talking about AC material, we focused on the adsorbents that were explicitly stating that they were activated carbon regardless of the source type (natural for example). A major example is the classification of the *Ziziphus jujuba*, since it can be allocated to the "natural adsorbents" or "AC" sections. However, it was chosen to be allocated to the AC group since it is carbonized and not used in its natural form. An adsorbent was classified as functionalized when the adsorbent is a composite material that has more than one classification. For natural adsorbents classification, the adsorbent can be slightly modified or in its natural form such as eggshells.

The majority of the adsorption experiments were through batch experiments. Firstly, stock solutions of HA were prepared in NaOH, which is then diluted to the desired concentration. A known weight of adsorbent is measured (dosage) and placed in an Erlenmeyer flask and the sample is then put into a shaker at a specified rotational speed, and temperature and left for some time, the concentration of the HA is then measured through various methods. The most widely used method for the determination of HA concentration in an aqueous solution is through UV–Visible spectrophotometry at a maximum wavelength of 254 nm, while others might use $\lambda_{max} = 400\text{-}440$ nm. Other methods of measuring the HA content are through TOC analysis. However, since the HA solution is of yellowish/brownish color [57], UV–Vis spectrophotometry would be a more popular way of determining the HA concentration in aqueous media.

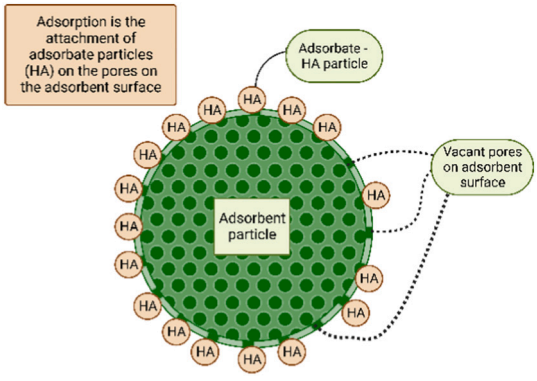

Fig. 7. The adsorption of HA on the adsorbent surface.

3.1. Activated carbon and carbon-based adsorbents

Activated carbon (AC) is a highly porous carbon material that is used for the adsorption and removal of pollutants due to its large surface area and high porosity [58]. AC can be used in water treatment for the removal of HA using adsorption, where the AC samples can be obtained commercially or can be synthesized through the activation of carbon-source materials. Two commercial ACs from bituminous coal which are Cullar D (Cm1), and Hydraffin 30 N (Hm1) were studied for the removal of HA from wastewater [8]. Maximum removal capacities of Cm1 (0.146 mg/g) and Hm1 (0.135 mg/g) of HA were achieved at 35 °C, with initial HA concentrations of 7 mg/L and 10 mg/L respectively at a pH of 4.5. The adsorption of HA on Cm1 and Hm1 relied heavily on initial HA concentration and was characterized as an exothermic process [8]. The adsorption capacity of Cm1 and Hm1 were relatively low compared to other adsorbents such as commercially bought AC, which was able to achieve a HA removal capacity of 29.7 mg/g at conditions listed in Table 1 [59]. Moreover, the AC was regenerated through ultrasonic treatment for 5 cycles, optimally at pH = 10, ultrasonic frequency of 37 kHz for 60 min and after the 5th cycle, the capacity was reduced by 1.86 %. This shows the AC's viability and effectiveness in removing HA since the regeneration of the adsorbent allows for a better cost-effective process if it is to be implemented at the industrial scale. *Ziziphus jujuba* is an agricultural waste product, it was utilized to synthesize AC and then treated with nitric acid to be used for the adsorption of HA from water [60]. The adsorption of HA via the *Ziziphus jujuba* was an endothermic and spontaneous process, where it followed pseudo-second-order kinetics and the Langmuir isotherm. *Ziziphus jujuba* was able to achieve an optimal adsorption capacity of 76.92 mg/g, and the high adsorption capacity was attributed to the hydroxyl groups of carboxylic acids, alcohols and phenols on the surface, which were increased following the treatment by nitric acid [60]. In other studies, the adsorption behavior of HA coupled with heavy metals is analyzed. In the study by Chen et al., the cooperative adsorption of Cr(VI) and HA on powdered activated carbon (PAC) is studied [61]. The adsorption experiments showed a 16 % increase in HA adsorption with the presence of Cr(VI). Multiple mechanisms justified the enhanced adsorption capacity such as: (1) HA and Cr(VI) adsorbed on the surface via physical interactions between PAC and adsorbates, (2) HA and Cr(VI) reactions with the oxygen-containing compounds from PAC surface, and (3) electrons provided by the HA structure as well as PAC surface that reduce Cr(VI) to Cr(III) that form complexes with HA that adsorbs on PAC surface.

Activated carbon materials can also be coated or incorporated with iron particles, which in some cases enhance the adsorption of HA. According to Rashtbari et al., AC (prepared from worn-out tires) and AC coated with nano zero-valent iron (nZVI) were studied to observe the effect of having iron particles on the performance of the adsorbent in HA removal [62]. It was found that the HA adsorption capacity of AC (98.03 mg/g) was much greater than AC-nZVI (86.95 mg/g) at the same experimental conditions (highlighted in Table 1), despite the nZVI nanoparticles structure being abundant with pores that are capable of sequestering the HA particles. The main mechanism of adsorption for both adsorbents was found to be through the chemical sharing of electrons. The AC-Fe adsorbent was able to be regenerated for 5 cycles, however, the efficiency was found to decrease from 93.34 % to 72.69 %. The reduction in efficiency is attributed to the segments of HA that have undergone decomposition in the AC pores and therefore reduced the porosity of the AC [62]. In contrast, Godini et al. noted that the iron-coated AC (AC-Fe) achieved a greater capacity than AC alone and had an outstanding HA adsorption capacity of 60.72 mg/g in comparison with the 40.56 mg/g achieved by AC alone [63] (the AC source was not stated). Surface area is considered an important property of the adsorbent, since a higher surface area suggests the presence of active sites for the uptake of the adsorbate/pollutant, therefore, a higher surface area usually corresponds to a higher adsorption capacity and/or removal.

Table 1
List of all activated carbon and carbon-based adsorbents.

Adsorbent	BET surface area (m^2/g)	Capacity (mg/g)	Conditions (highest removal)	Isotherm model	Kinetic model	Adsorption mechanism	Reference
Cullar D (Cm1)	900	0.146	T = 35 °C, pH = 4.5, D = 10 g/L, $[HA]_i$ = 7 mg/L	Langmuir	Not reported	Hydrophobic interaction	[8]
Hydraffin 30 N (Hm1)	1050	0.135	T = 35 °C, pH = 4.5, D = 10 g/L, $[HA]_i$ = 10 mg/L	Freundlich	Not reported	Hydrophobic interaction	
Graphene (G)	Not reported	41.4	pH = 3, $[HA]_i$ = 10 mg/L, t = 10 min, D = 0.1 g/L	Freundlich	PSO	Electrostatic, hydrophobic, π-π inter. & hydrogen bonding	[65]
Graphene oxide (GO)	Not reported	39.3		Langmuir	PSO		
AC (worn out tires)	Not reported	98.03	D = 1.6 g/L, $[HA]_i$ = 50 mg/L, t = 45 min, pH = 2	Langmuir	PSO	Chemisorption	[62]
AC-nZVI	821.52	86.95		Langmuir	PSO	Chemisorption	
AC	Not reported	29.7	pH = 3, $[HA]_i$ = 10 mg/L, D = 0.1 g/L, t = 10 min	Not reported	Not reported	Physical	[59]
Dual-pore carbon shells (DPCS0.05)	1325	99.27	V = 50 mL, $[HA]_i$ = 50 g/mL, D = 25 mg, 150 rpm, T = 25 °C, t = 12 h	Langmuir	PSO	Not reported	[67]
Ziziphus jujuba	970	76.92	T = 20 °C, $[HA]_i$ = 50 mg/L, pH = 4-6, t = 300 min, D = 0.05 g	Freundlich	PSO	Chemisorption & physical	[60]
MWCNTs	270	31.37	pH = 4, t = 3 h, $[HA]_i$ = 20 mg/L, D = 0.6 g/L, T = 23.3 °C, 140 rpm	Freundlich	PSO	Not reported	[66]
AC-Fe	596	60.72	pH = 5, $[HA]_i$ = 30 mg/L, T = 28 °C, t = 18 h, V = 100 mL, 100 rpm	Not reported	Not reported	Pore diffusion & chemical reaction	[63]
PAC	1400-1600	Not reported	D = 20 mg/50 mL, $[HA]_I$ = 20 mg/L, pH = 3-11, T = 25 °C, 180 rpm	Not reported	Not reported	1. HA and Cr(VI) by competitive physical interaction 2. HA and Cr(VI) chemically bonded to oxygen-containing compounds 3. Electron provision for transformation to HA-Cr(VI) and HA-Cr(III) complexes.	[61]

Key: T = temperature, D = dosage of adsorbent, t = time, $[HA]_i$ = initial concentration of humic acid, V = volume of water.

The surface area of the AC (760 m^2/g) was greater than that of AC-Fe (596 m^2/g), so this could not be the reason for the enhanced capacity, however, it can be attributed to the presence of iron oxide that can lead to the formation of metal-ligand complexes with the HA structure. Moreover, the mechanism of adsorption was in agreement with what was achieved by Rashtbari et al. [62], and that was that the adsorption mechanism was governed by chemical reaction and pore diffusion [63]. The iron is usually added to include a magnetic property to the adsorbent for a better recovery of the adsorbent in the liquid phase if it is to be used more than once, as well as contribute to the adsorption of HA onto the surface of the AC.

Other carbon-based materials can also be utilized for the adsorptive removal of HA from wastewater. Graphene oxide (GO) is a carbon-based material that is synthesized from sheets of graphite that are oxidized through different methods (such as Hummer's method) and possesses desirable electrical, optical and chemical properties for adsorption and many other applications [64]. In a study conducted by Naghizadeh et al., the performance of graphene (G) and GO were compared, where GO was proven to be more effective in the removal of HA despite having a smaller capacity (39.3 mg/g) compared to G (41.4 mg/g) [65]. The reason why GO has a greater efficiency was not mentioned in the study, but it could be attributed to the functional groups present in GO structure in comparison with graphene structure alone which is mainly carbon. The adsorption mechanism was found to depend on electrostatic interaction, Vander Waals forces, π-π interrelation and hydrogen bonding, which in turn depends on the properties of HA and the adsorbent surface and their interaction [65]. Multi-walled carbon nanotubes (MWCNTs) were also investigated for the removal of HA from water [66]. The MWCNTs were able to achieve an adsorption capacity of 31.37 mg/g at a pH of 4, an initial concentration of HA of 20 mg/L, and an adsorbent dosage of 0.6 g/L. MWCNTs were considered good adsorbents due to their small size, effectively large surface area (270 m^2/g), crystalline form, unique network, and high reactivity [66]. A novel dual-pore mesoporous carbon shell (DPCS) was synthesized by Yu et al. and was investigated for the removal of HA from water [67]. During the synthesis of the DPCS, an additional layer of silica was added to prevent the aggregation of the carbon particles and to have good dispersity in water. The adsorption of HA using DPCS0.05 achieved the best results and efficiency of 94.2 %. The adsorption process followed pseudo-second-order kinetics and the Langmuir isotherm. Through adsorption studies, it was determined that the separation factor value (R_L value) ranged from 0.003 to 0.03 which is considered favorable [67].

When comparing all AC and carbon-based adsorbents, it was determined that the best adsorption capacity for HA was acquired using DPCS0.05 (99.27 mg/g). This was attributed to the presence of richer carboxylate groups compared to AC indicated by FTIR characterization. Moreover, the sodium ions carried by the carboxylate groups on the adsorbent promoted the removal of organic anions through interaction with those ions. DPCS is also an effective adsorbent due to its large surface area, thin carbon layer, dual-pore architecture, large pore volume and highly hydrophobic surface [67] which are all important properties that allow better adsorption capacity to be achieved.

3.2. *Clay-based adsorbents*

Natural and modified clays are considered competent adsorbents for the removal of a wide range of pollutants and are usually used in water purification and remediation of contaminated water. The main advantage of using clays as adsorbents or even incorporating them in the structures of adsorbents would be their high abundance and low costs [68]. To study the performance of natural clays in HA adsorption, Gueu et al. collected 3 different samples of clay from the Ivory coast denoted by D, Y and K that represent the cities in which these clays were obtained (Dabou, Yamoussoukro and Katiola respectively). Through characterization of the samples, clay "Y" was found to be composed of kaolinite and illite, while clays "D" and "K" were composed of kaolinite, illite and smectite [69]. The adsorption relied more on electrostatic interaction between the HA and the surface of the clay, ligand exchange as well as Vander Waals hydrophobic forces. Clay "Y" had the best capacity due to its crystalline structure that allowed efficient adsorption of HA and had

adsorbed 115 mg/g of HA at a pH of 3 [70].

Kaolinite is a clay mineral with a chemical formula of $Al_2O_3.2SiO_2.2H_2O$ and 1:1 alternating layers of uncharged dioctahedral layers. Each layer consists of a single silica sheet and single alumina octahedral sheet [71]. Al-Essa investigated the adsorption of HA from water using 3 types of kaolinite clay found in Jordan: KTD-Kaolinite, which is natural clay extracted from King Talal Dam (KTD) sediments, FHA-Kaolinite which is commercially bought kaolinite (Fluka company), and unmodified kaolinite (obtained from a quarry located in the south of Jordan). TGA analysis showed that upon the modification of the kaolinite, the clay becomes more thermally stable than before modification. Due to the higher O/C ratio of the humic acid fractions, FHA-kaolinite presented a higher percentage of removal of HA from water than KTD-kaolinite [72]. Kaolinite clay was also studied for the removal of HA from the water via a continuously packed column [53]. According to Heikal, optimal removals of HA were achieved at a pH of 1, a flowrate of 15 mL/min, a retention time of 30 min, and an initial HA concentration of 1 ppm [53]. The optimal capacity as well as the isotherm and kinetic studies were not highlighted in any of the studies presented previously for kaolinite. This is a gap that needs to be filled to predict the mechanism of adsorption as well as for comparison purposes.

Bentonite and montmorillonite are two types of mineral clays that can also be used for wastewater remediation. Bentonite is a type of clay that is characterized by 2 tetrahedral silica sheets and an octahedral aluminum sheet with a chemical formula of $Al_2H_2Na_2O_{13}Si_4$ [69], while montmorillonite has a chemical structure of $Al_2H_2O_{12}Si_4$ [73]. In the study mentioned previously conducted by Heikal, kaolinite was also compared to montmorillonite and Fe-modified montmorillonite (Fe-montmorillonite) for the removal of HA via column adsorption [53]. When comparing the performance of the Fe-montmorillonite and montmorillonite, it was found that the iron-modified clay had a better HA removal, which is due to the iron ions anchoring in the HA ions via complexation. Moreover, the Fe-montmorillonite was regenerated for 5 cycles which validates the economic viability and efficiency due to the reusability potential of the adsorbent. For the regeneration of the clay, it was filtered, then washed with distilled water then dried in the oven for 12 h at 100 °C, then undergoes calcination for 4 h at 300 °C. However, after the regeneration (5 cycles), the percentage removal of HA using Fe-montmorillonite slightly decreased from 99 % to 97.2 % [53] which is a good indicator of the regeneration ability of this adsorbent. Bentonite and montmorillonite nanoparticles were synthesized and experimented for the removal of HA from water [74]. Optimal adsorption of HA using bentonite (58.21 mg/g) and montmorillonite (48.2 mg/g) nanoparticles was achieved at a pH of 3, initial HA concentration of 40 mg/L and dosage of 0.25 g/L. The adsorption process followed the Freundlich isotherm and pseudo-second order kinetics, where the adsorption kinetics was shown to occur in two consecutive steps: initially, fast adsorption of the adsorbent on the external surface, followed by slow and gradual adsorption until the process reaches its equilibrium [74]. Correspondingly, there are many unconventional types of clays that can be utilized as adsorbents, and it depends on the abundancy of clay at a specific geographic location. For instance, attapulgite is a type of clay that is found in China abundantly and is considered a one-dimensional material with a unique structure [75]. Modified attapulgite was used for the removal of HA from water, where three modification techniques were compared: acid activation, sodium modification and heat activation. Batch adsorption studies were utilized for evaluating the effectiveness of the adsorption, where the study was performed at a neutral pH, 50 mg of the adsorbent, and an initial HA concentration of 10 mg/L. It was suggested that the best activation method was acid coupled with sodium organic modification, which was followed by modification/activation through microwave [75]. Other types of clay that can be utilized for HA removal from groundwater is vermiculite/palygorskite [43]. The vermiculite/palygorskite was used for the simultaneous removal of HA and ammonia, and from adsorption experiments, it was determined that the HA was removed more efficiently by the palygorskite while the ammonia was best removed by the vermiculite. The HA removal was a spontaneous and exothermic process, and the mechanism of adsorption was mainly physical, and the adsorption conditions are mainly highlighted in Table 2. Efficient removals of both ammonia and HA (80-90 %) were evident using vermiculite/palygorskite as adsorbent since the final concentration of HA reached values below the regulatory limit for groundwater. The mechanism of HA adsorption was described as physical, and it was evident that since clay minerals are negatively charged, the presence of functional groups such as phenols and carboxylic groups will not enhance or prevent the electrostatic interaction between the adsorbent and adsorbate.

All in all, despite clay structures being naturally negatively charged, they were somewhat effective in HA removal from wastewater, and that is because most of the clays are modified and would have positively charged functional groups that would attract the negatively charged HA and facilitate adsorption. An example of this is the Fe-montmorillonite adsorbent; upon the modification of the montmorillonite, the adsorption of HA was enhanced due to the presence of iron which enhanced the ligand complexation of the HA structure. The clay that attained the best adsorption capacity was clay "Y", with a capacity of 115 mg/g. This is probably due to having more than one adsorption mechanism as well as the sample being composed of different types of clays (not just one type). However, the regeneration ability needs to be addressed for clay-based adsorbents as they can be a cost-effective mode of adsorption.

3.3. Zeolite/resin adsorbents

Zeolites are mainly used for ion-exchange applications but some are considered effective adsorbents for the treatment of groundwater, wastewater and drinking water. Zeolites can be classified into two types: natural and synthetic, and they are classified as porous aluminosilicates with crystalline structures [76]. Orha et al. compared a natural silver-doped zeolite (ZN-Ag), MWCNTs and ZN-Ag (MWCNT-Z Ag) and a silver-doped synthetic zeolite (ZA-Ag) for their performance of HA (5-25 mg/L) removal from the water via adsorption [77,78]. The adsorption conditions in these studies were in batch conditions at a volume of 100 mL, initial HA concentrations of 5-25 mg/L, a dosage of 0.2 g of each adsorbent, a temperature of 25 °C, a pH of 4-5, and kept for 1-180 min. Through isotherm studies, it was found that the adsorbents fitted the Langmuir and Dubinin-Radushkevich (D-R) isotherms. It was determined that ZA-Ag had the greatest adsorption capacity (47.9 mg/g), followed by MWCNT-Z Ag (20.2 mg/g) and then ZN-Ag (2.4-6.9 mg/g). No specific reason for this trend was determined by the author. Kinetic analysis showed that the adsorption followed PSO kinetics [77,78]. The adsorption mechanism of the natural and synthetic silver-doped zeolites (ZN-Ag and ZA-Ag) was found to be physical [78]. For the natural, silver-doped zeolite, there was a discrepancy in the values reported for optimal capacities. This can be because the values in [78] were mainly dependent on results from isotherm models (Langmuir), while in [77], the data was obtained via experimentation and not theoretical data, however, as shown by both studies, the modified zeolites (whether natural or synthetic) presented greater performances in the removal of HA from the water via adsorption. Modified zeolites are also proven to be competent HA adsorbents, such as demonstrated by Wang et al. where ZnO-30N zeolite was able to remove HA completely from wastewater [79]. The authors also demonstrated the effect of having Cr (VI) along with HA and its effect on the adsorption of HA. It was found that the presence of Cr facilitates the adsorption of HA on the zeolite, this is due to the HA forming complexes with the Cr and making it easier to remove, where the zeolite reached a maximum capacity of 34 mg/g at a faster rate than with HA alone in water [79]. This suggests that having Cr present in the water enhances the HA removal as well due to complexation, although Cr in water is unfavorable but having both pollutants in water can help simultaneously remove HA by this adsorbent. In a similar study, ZnO-30N zeolite was compared with other adsorbents with different weight percentage loadings of the ZnO on the

Table 2
List of clay-based adsorbents.

Adsorbent	BET surface area (m^2/g)	Capacity (mg/g)	Conditions (highest removal)	Adsorption mechanism	Reference
Y-Na+	36.29	115	D = 1 g/L, pH = 3, T = 25 °C, $[HA]_i$ = 50 mg/L	Electrostatic, ligand and hydrophobic	[70]
Kaolin	10.05	Not reported	Fixed bed: $[HA]_i$ = 1 ppm, flowrate = 15 mL/min, t = 90 min, pH = 1	Not reported	[53]
Montmorillonite	Not reported	Not reported		Not reported	
Fe-montmorillonite	83.79	Not reported		Not reported	
Bentonite	210-250	58.21	$[HA]_i$ = 40 mg/L, pH = 3, T = 25 °C, D = 0.25 g/L	Not reported	[74]
Montmorillonite	Not reported	48.2		Not reported	
FHA-Kaolinite	12.8	Not reported	$[HA]_i$ = 10-150 mg/L, t = 24 h, T = 25-45 °C, pH = 4-6	Ligand interaction	[72]
KTD-Kaolinite	15.8	Not reported			
Unmodified kaolinite	33.5	Not reported			
Modified attapulgite	Not reported	Not reported	$[HA]_i$ = 10 mg/L, V = 100 mL, pH = 7, D = 50 mg, 400 rpm	Electrostatic attraction	[75]
Vermiculite/ palygorskite	Not reported	Not reported	Batch - D = 1-7 g in 100 mL, $[HA]_i$ = 20 mg/L, pH = 2-9, T = 20-60 °C, 200 rpm, t = 1-10 h. Continuous - [HA]I-10 mg/L, flowrate = 0.91 cm^3/min, residence time = 5.4 h	Physical	[43]

Key: T = temperature, D = dosage of adsorbent, t = time, $[HA]_i$ = initial concentration of humic acid, V = volume of water.

zeolite (10-30 %) [80]. The optimal HA adsorption capacity of the ZnO-30N zeolite (60 mg/L) was shown to be greater than the ones reported by Wang et al. (34 mg/L), this could be due to the competition that is imposed by the Cr (VI) ions that hinder the adsorption of HA. The mechanism of adsorption was confirmed to be through electrostatic interaction between the negative HA functional groups and the positively charged ZnO-coated zeolite surface, this was followed by π-π stacking interactions in the second layer of HA adsorption. It was evident that the modification of the zeolite with nitric acid enhanced the HA adsorption due to more positively charged functional groups on the adsorbent surface that enhance the possibilities of adsorption. Furthermore, the weight percentage of the ZnO loading was proven to contribute to the adsorption quality, as the loading of ZnO increased from 10 to 30 %, the surface area consequently increased from 1.595 m^2/g to 6.199 m^2/g which also contributes to the enhanced adsorption capacity (availability of sites) [80].

Permanent magnetic anion exchange resins (MAER) were evaluated for the adsorption of HA which was synthesized by polymerization of glycidyl methacrylate monomer and crosslinking diallyl itaconate (DAI) and divinylbenzene [81]. The adsorption of HA by MAERs was found to be spontaneous, endothermic, and thermodynamically favorable, where the dominant mechanism was chemosorption due to the high value of enthalpy. By varying the DAI content from 1 to 15 %, the adsorption capacity of the MAER was enhanced from 2.57 to 3.14 mmol/g (this corresponds to approximately 584 mg/g to 713 mg/g, taking the molecular weight of 227 g/mol [82]) which was attributed to the increase in moisture content which aided in HA adsorption. The optimal capacity was reported to be 51 mg/g at the highest DAI concentration, this could also be explained due to the high surface area of MAER-3 (1.785 m^2/g) compared to MAER-2 (1.396 m^2/g) and MAER-1(1.109 m^2/g). Moreover, MAER was regenerated via a mixture of NaCl/NaOH (10 %/1 %), and the MAER with the highest DAI concentration had a regeneration capacity of 21 times. In addition to its superb regeneration abilities, MAER also presented excellent anti-fouling performance, which was taken back by reduced performance due to the loss of adsorption capacity through each progressive usage of the adsorbent. SEM investigations showed that the adsorption of HA caused a morphological change to the exterior of the resin surface. The monolayer adsorption by electrostatic interaction may turn into multilayer adsorption by physical forces as indicated by the Freundlich isotherm. FTIR showed that carbonyl groups may form hydrogen bonding with the un-ionized HA. The carbon atoms of -CH2-O- played important roles in the adsorption process [81].

Analogously, a novel hydrogarnet/zeolite composite was synthesized from a hydrothermally treated slurry of silica gel, alumina, calcium hydroxide and zeolite type A. Optimal conditions of adsorbent dosage of 50 mg in 20 mL, 25 °C and initial HA concentration of 30 ppm for 2 h attained a maximal capacity of 9 mg/g [83]. Zeolitic Imidazolate Framework – 8 (ZIF-8) was utilized in the removal of HA (50 ppm) from wastewater [84]. Π-π interactions and electrostatic interrelations could be possible adsorption mechanisms for HA, which were described as weak and reversible. The relatively low capacity of ZIF-8 (42.9 mg/g) was justified by the small pore diameter that makes the adsorbent pores difficult to access as well as the clustering of the adsorbent particles. The zeolite was regenerated for 4 cycles, where it was washed with cold water at 25 °C for 1 h. Washing with cold water did not improve efficiency, so hot water was used (85 °C) [84].

The adsorption process using fixed-bed reactors is also a very effective process for the removal of HA from water as demonstrated by Elsheikh et al. when studying the performances of natural zeolite (NZ), and surfactant (hexadecyltrimethylammonium bromide (HDMTA)) modified zeolite (SMZ) [85]. The adsorption conditions are presented in Table 3 and the desorption is done using ethanol solution as an eluent and 2 Bed volume per hour (BV/h) flowrate. The main adsorption mechanism was hydrophobic interaction and hydrogen bonding since a complete organic monolayer was observed. It was concluded that the HDMTA-modified zeolite with higher surfactant loading had a worse adsorption capacity than the natural zeolite, this was attributed to the formation of the bilayer and occupation of the pores which therefore results in a reduction of the surface area [85]. There are many advantages of continuous adsorption over batch processes, and therefore this area regarding HA adsorption needs to be further investigated and optimized to scale up the process and implement it on the industrial level.

3.4. Iron-based and magnetically retrievable adsorbents

Some adsorbents exhibit magnetic properties that can aid in the recycling and regeneration process due to their ability to be separated by applying an external magnetic field [86]. The addition of magnetic properties to these adsorbents has gained special attention due to its ease in investigating reusability as well as its enhanced adsorption properties

Table 3
List of zeolite/resin adsorbents.

Adsorbent	BET surface area (m^2/g)	Capacity (mg/g)	Conditions (highest removal)	Isotherm model	Kinetic model	Adsorption mechanism	Reference
ZnO-30N-zeolite	Not reported	34.157	D = 0.02 g, T = 25 °C, [HA]i = 35 mg/L, t = 15 min	Not reported	PSO	Electrostatic	[79]
Hydrogarnet/zeolite composite	120	9	D = 50 mg in 20 mL, T = 25 °C, $[HA]_i$ = 30 ppm, t = 2 h, pH = 7	Not reported	PSO	Not reported	[83]
Nano-ZIF-8	1400	42.9	S/L ratio = 2.5, t = 2 h, T = 20 °C, [HA]i = 50 ppm	Langmuir	PSO	Electrostatic & π-π interaction	[84]
MAER-3	1.785	51	pH = 11, T = 293 K, D = 1 g/L, $[HA]_i$ = 100 mg/L	Freundlich	PSO	Ion exchange	[81]
SMZ	11.83	28	T = 25 °C, pH = 10, t = 20 min, [HA]I = 6 mg/L, HDMTA loading = 75 %, Flowrate = 2 BV/h	Not reported	Not reported	Hydrogen bonding & hydrophobic interaction	[85]
ZnO-30N-zeolite	6.199	60.3	D = 50 mg, V = 25 mL, $[HA]_i$ = 140 mg C/L, 50 rpm, T = 21 °C, pH = 3-9.5	Not reported	PSO	Electrostatic attraction	[80]
MWCNT-ZAg	Not reported	20.242	D = 0.2 g, T = 25 °C, t = 180 min, pH = 4, V = 100 mL, $[HA]_i$ = 5-25 mg/L	Langmuir	PSO	Physical	[77]
ZN-Ag	Not reported	2.42		Langmuir	PSO	Physical	
ZA-Ag	Not reported	46.8603	V = 100 mL, $[HA]_i$ = 20 mg/L, D = 0.2 g, T =	Not reported	PSO	Physical	[78]
ZN-Ag	Not reported	6.9199	25 °C, t = 120 min, pH = 4.	Not reported	PSO	Physical	

Key: T = temperature, D = dosage of adsorbent, t = time, $[HA]_i$ = initial concentration of humic acid, V = volume of water.

of HA and other pollutants. Nano-zero valent iron has also proven its applicability in electrochemical wastewater treatment applications of phenolic wastewater [87], this shows its great potential in the wastewater treatment industry. Therefore, this subsection was added to highlight the importance of these properties in an adsorbent's performance.

A novel adsorbent of Mg/Al-LDH with magnetic biochar on poplar sawdust ($CoFe_2O_4$@PBC-LDH) and bamboo powder ($CoFe_2O_4$@BBC-LDH) was developed for the removal of HA from wastewater. The adsorption of HA onto these adsorbents was governed by ion exchange and electrostatic attraction, and the reaction was endothermic but spontaneous. The capacities exhibited by $CoFe_2O_4$@PBC-LDH were 240.58 mg/g, while for $CoFe_2O_4$@BBC-LDH it was 337.83 mg/g. It is evident that the BBC adsorbent was able to withhold more HA, and this was attributed to the greater surface area of the BBC (178.779 m^2/g) compared to PBC (116.095 m^2/g). Both adsorbents were able to be regenerated for seven cycles where the capacities were still maintained at high levels [88]. Similarly, the novel $FeNi_3/SiO_2/TiO_2$ magnetic nanocomposite was able to reduce the HA concentration (5 ppm) by 94.4 %, which corresponds to a capacity of 138 mg/g of HA, at a pH of 3 and adsorbent dosage of 0.1 g/L. The high adsorption capacity is attributed to the high surface area and pore volume (481 m^2/g and 0.2 cm^3/g, respectively) [89].

Activated carbon (AC) was prepared from sawdust, then magnetized by Fe_3O_4, coated by SiO_2 and functionalized by 3-aminopropyltrimethoxisilane (APTMS), the adsorbent was denoted by AC/Fe_3O_4@SiO_2-APTMS and was used for the adsorption of HA from water [52]. Normally this would be classified as an AC, but the outstanding feature of this adsorbent is its magnetic property. Adsorption was endothermic and spontaneous, and the optimal adsorption conditions are shown in Table 4 which resulted in an adsorption capacity of 20.57 mg/g. It was observed that AC had a greater BET surface area (1629.6 m^2/g) compared to AC/Fe_3O_4@SiO_2-APTMS (534.43 m^2/g) which was explained by the blocking of the pores by the Fe_3O_4 particles. The adsorbent was regenerated using sodium hydroxide and was effective for 4 cycles where the efficiency decreased from 97.85 % to 65.28 % because the functional groups are degradable and active carbon sites are reduced [52]. During the regeneration of the adsorbent, the magnetic feature was useful in removing the adsorbent effectively with minimum losses, which is beneficial from an economic perspective.

Shu et al. studied the performance of maghemite-incorporated hydroxyapatite (HAP/γ-Fe_2O_3) as an adsorbent for the removal of HA from water [90]. Batch adsorption experimentation was carried on by varying pH from 3 to 10, 180 rpm, initial HA concentration between 20 and 80 mg/L, an adsorbent dosage of 0.1 to 3 g/L, and temperatures between 298 and 313 K. Through characterization – FTIR in particular – it was shown that the maghemite did not present considerable change in the chemical structure of HAP and the adsorption mechanism was completely interpreted as a physical [90].

Magnetic nanoparticles (Fe_3O_4 NP) were synthesized from sand and studied for the removal of HA from Indonesian peat water [50]. Batch experiments were done in a thermostatic shaker by varying the temperature from 25 to 55 °C, pH from 2 to 12 and operation time from 1 to 240 min, where equilibrium was attained at 90 min. The optimal capacity of Fe_3O_4 NP for HA adsorption was found to be 43.32 mg/g, where the adsorption fitted the Sips isotherm and PSO kinetic models. The adsorption of HA on the nanoparticles was non-spontaneous and endothermic [50]. Another adsorbent was synthesized from an oyster shell and was supported by nano zero-valent iron nanoparticles (nZVI) for the removal of HA (5 mg/L) from water [91]. Characterization studies showed that the main elements present on the surface were Ca, O, Fe, Na, and lime. The BET surface area was 16.85 m^2/g which is fairly low compared to other adsorbents. Adsorption of HA on oyster shell – nZVI fitted the Freundlich isotherm best as well as PSO kinetics, where the optimal adsorption capacity was noted to be 0.96 mg/g [91]. Pourbaghaei et al. were able to fabricate a composite material of nZVI and chitosan biopolymer (nZVI/chitosan) for the adsorption of HA and nitrate from wastewater [92]. Optimal HA removal was found to occur at a pH of 5.5, dosage of 0.098 g, 27 min contact time, and initial HA concentration of 30 mg/L, where 98.1 % removal of HA occurred. The adsorption was governed by chemisorption, van der Waals interaction as well as electrostatic interactions between the negatively charged $RCOO^-$

Table 4
Iron-based and magnetic adsorbents for humic acid removal.

Adsorbent	Capacity (mg/g)	Conditions (highest removal)	Isotherm model	Kinetic model	Mechanism	Reference
PANI-coated mask	11.11	D = 10 g/L, pH = 2, $[HA]_i$ = 50 mg/L, t = 1 h	N/A	PSO	Chemisorption	[96]
Polyaniline (PANI)	N/A	D = 1.75 g PANI in 5 mL water, $[HA]_i$ = 200 mg/L, pH = 8	N/A	N/A	N/A	[95]
PANI-/H-TNB	339.46	pH = 5, T = 298 K, D = 0.3 g/L, t = 24 h	Langmuir	PSO	Chemisorption	[97]

KEY: T = temperature, D = dosage of adsorbent, t = time, $[HA]_i$ = initial concentration of humic acid, V = volume of water.

groups in the HA and the positively charged NH_3^+ in the chitosan biopolymer surface. nZVI/chitosan underwent 4 cycles of regeneration at minimum efficiency losses, where the adsorbent was magnetically retrieved. The adsorbent also presented anti-bacterial properties, which could be useful in wastewater treatment.

Wu et al. studied $Fe@Fe_2O_3$ nanowires that were used for the removal of HA from water under anoxic conditions [93]. Optimal adsorption (65.51 mg/g) was achieved at a pH of 6 and room temperature. In anoxic removal, the solutions are purged with argon gas to remove the oxygen and then the adsorbent is added [93].

3.5. Polyaniline-based adsorbents

Polyaniline (PANI) is a conductive polymer synthesized through chemical/electrochemical methods using aniline, HCl and ammonium persulfate. It is used as a conductor in many fields such as nanotechnology for the development of sensors, as well as anti-corrosion applications due to its low cost, easy synthesis, and high environmental stability [94]. PANI was utilized in conjunction with other sheets and fibers to aid the adsorption of HA from wastewater, as well as regenerating and re-using it as a conductor. Yeap et al. observed that 89.5 % of the HA content was removed at an optimum dosage of 1.75 g PANI in 5 mL of water and an initial HA concentration of 200 mg/L. Regardless of the excellent uptake of HA by the PANI, the electrical conductance of the used PANI sheets was reduced by 14 times in comparison to fresh PANI sheets. Therefore, as more HA adsorbs on the adsorbent surface, the conductance of the PANI sheet decreases and hence reduces the chances of reutilizing it as a conductor [95]. In an analogous study, facial sheet masks were modified with PANI and used for HA adsorption as well as a possible electrical conductor [96]. The PANI-coated mask was found to be effective in HA removal (83.1 % removal). However, the use of the mask as a conductor could not be evaluated due to no conductance value obtained for such low loading of PANI (10 g/L), and at low pH's the HA was observed to precipitate and form sludge, which requires an extra cost to treat and is not very feasible [96]. Polyaniline/hydrogen-titanate nanobelt composite (PANI/H-TNB) was synthesized and evaluated for the simultaneous removal of HA and Cr (VI) from wastewater [97]. It was found that >92 % of the natural organic matter (NOM) was removed from drinking water in the Inner Mongolian area using this adsorbent, as well as achieving a superb HA capacity of 339.46 mg/g using the conditions highlighted in Table 5. The adsorption of HA was mainly through surface complexation between the disassociated HA macromolecules and the positively charged PANI. According to kinetic studies, the dominating mechanism is chemisorption. PANI/H-TNB was regenerated for 10 cycles, where a small decrease in the capacity was noted and this was justified by the incomplete desorption from the surface of the adsorbent [97]. Future studies should target the use of PANI for electrical conducting usage, which would give this adsorbent double benefit, removal of HA and conductance of electricity.

3.6. Functionalized adsorbents

To increase the effectiveness of an adsorbent, other functional groups are added to target the removal of certain pollutants from water. Functional groups can be added in order to enhance certain properties of the adsorbent such as mechanical strength. Santosa et al. synthesized an adsorbent that is a composite of magnetite (Fe_3O_4) and Zn/Al layered double hydroxide (LDH) for the adsorption of HA from wastewater. The best adsorption capacity (35.28 mg/g) occurred at a pH of 4 and was governed by electrostatic interaction. The use of Fe_3O_4-Zn/Al LDH adsorbent for water treatment was proven better than commercially used alum since a dosage of 10 mg of adsorbent in 5 mL of water completely removed the color exhibited by HA [98]. In comparison with Zn-Al LDH without the magnetite, Flake Zn-AL LDH (FLDH) and microspheres LDH (MLDH) were compared for HA (25 mg/L) adsorption. The FLDH exhibited superior adsorption capacity (84 mg/g) compared with MLDH (60 mg/g), this was attributed to the surface properties of the adsorbent and their interaction with HA. The adsorbents were successfully regenerated for 5 cycles using potassium nitrate solution, where the adsorbents experienced <20 % efficiency reduction. The decrease in efficiency is attributed to the gradual damage of the crystal structure of the LDH with continuous mixing [99]. When comparing both adsorbents, it can be said that the modification of the Zn-Al with magnetite decreases the adsorption capacity of the HA, this can be due to the agglomeration of these particles or reduced surface area or pore volume. In another study, the magnetite was also modified with hyperbranched polyethyleneimine (HPEI) and then used as an adsorbent for HA removal. Fe_3O_4@HPEI nanoparticle concentration was optimized using the Box-Behnken design tool, where it optimally adsorbed 97.27 % of the HA (79 mg/L) at a pH of 3 and a dosage of 0.128 g/L. Regeneration studies carried out using 0.1 mol/L NaOH and deionized water, Fe_3O_4@HPEI exhibited high removal efficiency even after 4 cycles (82.83 %) [100].

Zhang et al. synthesized a fibrous adsorbent that is a combination of cellulose acetate (CA) and chitosan fibers (CS) for the removal of HA from wastewater. The electro spun CA/CS adsorbent exhibited excellent mechanical properties such as its uniform morphology and high tensile strength as well as a high adsorption capacity of 238.10 mg/g. The

Table 5
Polyaniline based adsorbents for humic acid removal.

Adsorbent	BET surface area (m^2/g)	Capacity (mg/g)	Conditions (highest removal)	Isotherm model	Kinetic model	Mechanism	Reference
$FeNi_3/SiO_2/TiO_2$	481	138	pH = 3, $[HA]_i$ = 5 mg/L, t = 90 min, D = 0.1 g/L.	Langmuir	PSO	Not reported	[95]
CoFe2O4@PBC-LDH	116.095	240.58	T = 25 °C, pH = 3, D = 10 mg, t = 20 min	Freundlich	PSO	Ion exchange & electrostatic	[88]
CoFe2O4@BBC-LDH	178.779	337.83		Freundlich	PSO	Ion exchange & electrostatic	
AC/Fe3O4@SiO2-APTMS	534.43	14.6775	$[HA]_i$ = 30 mg/L, pH = 3, D = 2 g/L, t = 25 min	Langmuir	PSO	Not reported	[52]
HAP/γ - Fe2O3	100.5	54.95 (F) 601.91 (S)	pH = 7.5, 180 rpm, $[HA]_i$ = 20-80 mg/L, D = 1 g/L, T = 313 K	Freundlich & Sips	PSO	Electrostatic attraction	[90]
Fe3O4 nanoparticles	207	43.32	D = 0.1 g, V = 50 mL water, $[HA]_i$ = 10 mg/L, t = 90 min, T = 25 °C, pH = 2	Sips	PSO	Physical	[50]
Oyster shell nZVI	16.85	0.96	$[HA]_i$ = 5 mg/L, D = 0.5 g/100 mL, pH = 5, T = 40 °C, t = 90-120 min	Freundlich	PSO	Chemisorption	[91]
nZVI/chitosan		63	pH = 5.5, D = 0.098 g, t = 27 min, $[HA]_I$ = 30 g/L, $[NO_3^-]_I$ = 110 g/L	Freundlich	PSO	Chemisorption, van der Waals and electrostatic	[92]
Fe@Fe2O3 core-shell	31.1	65.51	pH = 6, T = room temp, $[HA]_i$ = 40 mg/L, D = 0.3 g/L, V = 50 mL	Langmuir	PSO	Electrostatic attraction	[93]

Key: T = temperature, D = dosage of adsorbent, t = time, $[HA]_i$ = initial concentration of humic acid, V = volume of water.

adsorption process was facilitated by electrostatic interactions and was found to be an exothermic process, and it was non-spontaneous [101]. Furthermore, a modified version of the CA/CS adsorbent incorporated cellulose nanocrystals (CNC) via a one-step co-axial electrospinning (CS/CA-CNC) [102]. The modified adsorbent exhibited smaller diameters, greater homogeneity and better mechanical properties, while the HA adsorption capacity was slightly compromised (151.41 mg/g). The HA adsorption was facilitated by electrostatic adsorption between the deprotonated HA carboxylic groups and protonated nitrogen-containing groups of chitosan [102]. The cotton-Linter-based adsorbent was fabricated from dimethyl aminoethyl methacrylate (DMAEMA) then quaterinized and protonated to produce QCL and PCL adsorbents for HA removal [49]. The adsorbent-HA interaction was dependent on electrostatic interactions, where maximum capacities of QCL (333 mg/g) and PCL (250 mg/g) were exhibited at 30 °C, pH of 6 and in a contact time of 24 h. It was realized that QCL adsorbent was more efficient than PCL due to the higher rate constant and adsorption rate. Desorption experiments were performed, where the highest desorption efficiency (75.98 %) was performed using 3 M NaOH and was governed by ion exchange [49].

Garnet media was modified with ferric chloride and was compared with unmodified garnet for its performance in adsorbing HA from water [103]. Both adsorbents showed good chemical and physical stability, however, the performance of the adsorption capacity of the modified garnet was 11-24 times better than the unmodified garnet, and the conditions for these are presented in Table 6. The enhanced performance was attributed to the modified garnet's surface roughness and positive charge of the surface due to Fe_2O_3 which is hydroxylated to form carboxylic groups that easily bind with the functional groups present on the HA. Through characterization, it was also proved that the surface area of the modified garnet was approximately 2 times greater than the unmodified one. This is because the modified garnet has a rougher surface with more pits and pores than the modified ones [103], and a greater surface roughness contributes to a lower contact angle [104], this suggests a higher wettability of the adsorbent surface and therefore greater adsorption since more of the HA is in contact with the surface. Minowa and Maeda prepared a composite of hydrogarnet and poly (lactic acid) using an electrospinning technique for the removal of HA from water [105]. Optimal adsorption capacities of HA (4.6 mg/g) were achieved using 10 mm × 10 mm in 10 mL, pH 7 and an initial HA concentration of 7 ppm for 24 h. In another study, hydrogarnet was prepared from blast furnace slag which is derived from steel and iron production plants. The blast furnace slag underwent a hydrothermal reaction that converted the slag into hydrogarnet structure used as an adsorbent for the removal of HA from water [106].

In another study, nano-MgO particles were proven as an effective 2-in-1 adsorbent and coagulant of HA from water [107]. The adsorbent was much more effective than AC due to its high surface area (66.83 m^2/g) as well as its superb HA removal capacity (1260 mg/g) that was 76 times greater than AC, as well as its high regeneration ability of 10 cycles through annealing at 500 °C. The excellent adsorption capacity is attributed to the rapid hydrolyzation of MgO, this means that $Mg(OH)_2$ which is only soluble in neutral or acidic conditions was soluble. HA is considered to have weak acid structures, so when MgO is dissolved in water, it releases the Mg^{2+} ions which serve as a multivalent cationic coagulant that facilitates HA removal [107]. Despite the high adsorbing capacity of nano-MgO particles, it can be observed that the regeneration of this adsorbent requires a very high temperature which can be considered quite costly/expensive.

Jarvis and Majewski reported the usage of plasma polymerized allylamine (ppAA) coating on the surface of quartz particles [108–110] for the removal of HA from water. The optimal adsorption capacity of ppAA coated quartz particles was determined to be 0.055 mg/g, at an initial HA concentration of 10 mg/L, dosage of 1 g in 10 mL, pH of 7 and contact time of 30 min [109,110]. The adsorbent was also able to be regenerated when rinsed with a pH 5 MilliQ solution, followed by adding 10 mL of pH of 11 MilliQ solution for 30 min and was able to achieve 4 cycles [109]. Several parameters affected the performance of this adsorbent in removing HA from water; polymerization time, plasma power, and allylamine flowrate [108–110]. Moreover, it was noted that the ppAA film age did not affect the performance of the adsorbent [109]. The adsorption mechanism was classified as the electrostatic attraction between the adsorbent surface and HA functional groups, since the amine groups on the ppAA coated quartz particles are protonated and

Table 6
List of functionalized adsorbents for humic acid removal.

Adsorbent	Capacity (mg/g)	Conditions (highest removal)	Isotherm model	Kinetic model	Mechanism	Reference
Fe3O4-Zn/Al LDH	35.28	D = 10 mg, V = 5 mL of water, pH = 4	Langmuir	PSO	Electrostatic	[91]
CA/CS nanofibers	238.1	pH = 4, D = 0.0011 g, V = 20 mL, t = 90 min, T = 25 °C, $[HA]_i$ = 30 ppm	Langmuir	PFO	Electrostatic	[101]
CS/CA-CNC	151.41	Ph = 4, D = 1.2 mg/20 mL, $[HA]_i$ = 30 ppm, 155 rpm, T = 25 °C.	Not reported	Not reported	Electrostatic	[102]
PCL	250	D = 0.05 g, t = 24 h, T = 30 °C, pH = 6	Langmuir	PSO	Chemisorption	[49]
QCL	333		Freundlich	PSO		
Fe3O4@HPEI	476.2	$[HA]_i$ = 79 mg/L, D = 0.128 g/L, pH = 3, t = 29 min	Freundlich	PSO	Chemisorption	[100]
FLDH	84	T = room temp, pH = 7, D = 0.5 g/L, $[HA]_i$ = 25 mg/L	Langmuir	PSO	Ligand & ion	[99]
MLDH	60		Langmuir	PSO	exchange	
Garnet	0.001	V = 100 mL, adsorbent volume = 50 mL, t = 3 h, speed = 100 rpm, T = 26 °C, pH = 7	Freundlich	Not reported	Physical	[103]
Modified garnet	0.02206		Langmuir and Freundlich	Not reported	Not reported	
Hydrogarnet/poly (lactic acid)	4.6	10 mm × 10 mm, V = 10 mL, pH = 7, $[HA]_I$ = 7 ppm, t = 24 h	Not reported	Not reported	Not reported	[105]
Blast furnace hydrogarnet	192.3	pH = 7, [HA] = 0-30 mg/L, t = 24 h	Freundlich	Not reported	Not reported	[106]
Nano-MgO	1260	$[HA]_i$ = 354 mg/L, pH = 6, D = 0.2 g/L, t = 24 h, V = 20 mL	Freundlich	Not reported	Not reported	[107]
ppAA coated quartz	0.055	$[HA]_i$ = 10 mg/L, V = 10 mL, D = 1 g, t = 30 min, pH = 7	Not reported	Not reported	Electrostatic attraction	[110]
ppAA coated quartz	Not reported	$[HA]_i$ = 10 mg/L, pH = 7, D = 1 g, V = 10 mL, t = 30 min	Not reported	Not reported	Electrostatic attraction	[109]
ppAA coated quartz	Not reported	$[HA]_i$ = 20 mg/L, pH = 5, D = 1 g, V = 10 mL, t = 30 min	Not reported	Not reported	Electrostatic attraction	[108]

KEY: T = temperature, D = dosage of adsorbent, t = time, $[HA]_i$ = initial concentration of humic acid, V = volume of water.

positively charged at values below the isoelectric point [109]. The studies by Jarvis and Majewski heavily shed the light on the effect of varying synthesis conditions of the adsorbent on the adsorption process rather than general operating parameters of the process, which is vitally needed in evaluating the effectiveness of such adsorbent. Nevertheless, there is a need to mention that the adsorption capacity attained by these adsorbents was noticeably lower than that of other functionalized adsorbents discussed in this section.

3.7. Natural adsorbents

Some materials inherently found in nature can be used as adsorbents without modification for the removal of several pollutants including humic acids from wastewater. These adsorbents are often referred to as "green" adsorbents since they originated from low-cost materials and are often sourced from agricultural sources, by-products, residues, or even wastes, as well as other low-cost sources [111], this section will highlight such adsorbents. Raw pumice stone as well as pumice modified with several acids including acetic acid ($C_2H_4O_2$–MP), hydrochloric acid (HCl-MP), phosphoric acid (H_3PO_4–MP), sulfuric acid (H_2SO_4–MP) and nitric acid (HNO_3–MP) [112]. According to the adsorption studies undergone, the modification of pumice stone with sulfuric acid attained the greatest adsorption capacity of HA (65.71 mg/g) compared to raw pumice stone (38.22 mg/g). It was also observed that the modification of pumice stone with acids enhanced the capacity and effectiveness of HA removal due to the effect of the acids on the surface of the adsorbents, including the enhancement of the surface area and pore volumes [112].

Another type of "green" adsorbent was studied by Zhang et al. for the removal of HA from water using modified aged refuse (MAR) [113]. Aged refuse is defined as the substance formed when the landfill refuse reaches a steady state, and no more decomposition occurs. According to Zhang et al., optimum HA capacity (29.18 mg/g) was achieved at a dosage of 2 g/L, pH of 8 at a temperature of 25 °C and for 120 min. The adsorption mechanism was governed by two aspects: physical by porous structure as well as chemical adsorption by ions and proton exchange between active sites of hydroxyl groups and other functional groups [113].

A powdered eggshell was also used as an adsorbent for HA removal from peat water [114]. Eggshell is commonly known for having carbonate materials as part of their chemical structure, which was backed up through IR spectra and other characterization analyses. The optimal adsorption conditions were defined in Table 7, where the adsorbent was able to achieve a capacity of 126.58 mg/g, which is considered high compared to other "green" adsorbents such as the MAR and modified pumice stones. Desorption studies were used to evaluate the regeneration and recyclability of the eggshell, where the saturated adsorbent was gently washed with distilled water, then loaded with 50 mL of HCl at different concentrations for 120 min. It was evident that as the concentration of the eluent was increased from 0.001 to 0.1 M the amount of desorbed HA also increased. This is justified by the increase in repulsive electrostatic forces between the protonated adsorbate (HA) and the adsorbent (eggshell powder) [114]. Powdered eggshell was also investigated by Mehri et al. for the adsorptive removal of HA from water [115]. The eggshell powder adsorbent was prepared using an incubator at 105 °C and 12 h. Adsorption experiments were carried out at variable pH between 4 and 10, contact time between 1 and 80 min, and dosage of 4-6 g/dL. The adsorbent was regenerated 10 times, however, there was a great reduction in efficiency (from 100 % to 60 %). The adsorption of HA was governed by ion-exchange, chemical and electrostatic interaction, as well as chelation and intra-particle diffusion [115]. The adsorption capacity was found to be 101 mg/g of HA which is lower than what was achieved in the study by Zulfikar et al. [114] which could be attributed to the preparation of the adsorbent itself.

It is beneficial to include such low-cost adsorbents for the removal of pollutants from wastewater since it would be a way of recycling and reincorporation the waste in a useful manner, as well as reducing costs for the disposal and treatment of these waste products. This is especially evident in the MAR applications, as the population grows exponentially and swiftly, the amount of solid waste increases and therefore more landfills are needed. As a result, utilizing the aged refuse beneficially would be both environmentally and economically friendly.

4. Isotherm and kinetic models

4.1. Isotherm models

Isotherm studies are usually carried out by a batch reaction where the temperature is fixed, and the initial concentration of HA is varied. Important information can be found from these isotherms such as the maximum adsorption capacity of the adsorbent as well as the interaction of the HA with the adsorbent surface and whether the interaction at the surface is homogenous or heterogeneous. Two isotherms were found to be abundant in the literature reviewed which were Langmuir and Freundlich [116,117]. Table 8 summarizes the isotherm parameters data for the majority of the adsorbents reported in the literature and discussed in this paper. The data includes parameters for different isotherms such as Langmuir and Freundlich and their corresponding R^2 values.

4.1.1. Langmuir isotherm

The non-linear form of the Langmuir isotherm is demonstrated as [118]:

$$q_e = \frac{q_m\, b_0\, C_e}{1 + b_0\, C_e}$$

where q_e is the adsorption capacity at equilibrium conditions (mg/g), q_m is the maximum adsorption (mg/g), b_0 is the Langmuir constant (L/mg) (also referred to as K_L) and C_e is the equilibrium concentration of the pollutant (mg/L). The Langmuir isotherm assumes single-layer

Table 7
Natural adsorbents for humic acid removal.

Adsorbent	Capacity (mg/g)	Conditions (highest removal)	Isotherm model	Kinetic model	Mechanism	Reference
Raw pumice	38.22	t = 75 min, pH = 3, D = 7 g/L, $[HA]_i$ = 5 mg/L, T = 25 °C	Langmuir and Freundlich	PSO	Physical	[112]
HNO3-MP	57.31			PSO	Physical	
H2SO4-MP	65.71			PSO	Physical	
C2H4O2-MP	52.28			PSO	Physical	
HCl-MP	45.05			PSO	Physical	
Modified aged refuse (MAR)	29.18	D = 2 g/L, pH = 8, t = 120 min, T = 25 °C	Langmuir	PSO	Physical and chemisorption	[113]
Eggshell powder	126.58	pH = 2, D = 5 g, V = 50 mL, t = 60 min, T = 25 °C, 100 rpm	Freundlich	PSO	Electrostatic attraction	[114]
Eggshell powder	101	pH = 4, t = 60 min, $[HA]_I$ = 15 mg/L, D = 5 g	Langmuir	PSO	Ion exchange, chemisorption, chelation, intra-particle diffusion and electrostatic interaction	[115]

Key: T = temperature, D = dosage of adsorbent, t = time, $[HA]_i$ = initial concentration of humic acid, V = volume of water.

Table 8
Adsorption isotherm data for reported adsorbents.

Adsorbent	Isotherm	Freundlich isotherm			Langmuir isotherm		Reference
		K_F (mg/g) $(L/mg)^{1/n}$	n	R^2	K_L (L/mg)	R^2	
Cullar D (Cm1)	Langmuir	0.079	2.883	0.748	2.797	0.941	[8]
Hydraffin 30 N (Hm1)	Freundlich	0.048	2.519	0.983	0.484	0.957	
Fe_3O_4-Zn/Al-LDH	Langmuir	19,687	Not reported	0.9642	Not reported	0.9919	[98]
CA/CS nanofibers	Langmuir	9	2.58	0.94	0.15	0.99	[101]
PCL	Langmuir	9.331	1.939	0.9832	0.0042	0.9827	[49]
QCL	Freundlich	14.22	2.347	0.9914	0.0084	0.991	
Y-Na^+ (natural clay)	Langmuir	Not reported	Not reported	Not reported	0.049	0.9968	[70]
$FeNi_3/SiO_2/TiO_2$	Langmuir	66.42	1.808	0.79	1.18	0.954	[89]
Fe_3O_4@HPEI	Freundlich	879	1.65	0.93	0.7	0.78	[100]
CoFe2O4@PBC-LDH	Freundlich	49.476	2.416	0.986	0.15	0.969	[88]
CoFe2O4@BBC-LDH	Freundlich	81.75	2.31	0.983	0.244	0.962	
FLDH	Langmuir	23.31	3.78	0.8495	0.094	0.994	[99]
MLDH	Langmuir	16.11	4.28	0.8972	0.084	0.9997	
Nano-ZIF-8	Langmuir	16.478	2.252	0.963	0.741	0.997	[84]
AC/Fe3O4@SiO2-APTMS	Langmuir	11.19	5.85	0.5197	2.91	0.985	[52]
Modified garnet	Langmuir and Freundlich	0.899	0.804505	0.99	0.034	0.997	[103]
AC	Langmuir	5.61	1.46	0.993	Not reported	0.9967	[62]
AC-nZVI	Langmuir	12.95	1.72	0.9929	Not reported	0.9951	
Nano-MgO	Freundlich	106	1.757469	0.968	0.0421	0.605	[107]
Raw pumice	Langmuir and Freundlich	1.163	1.5625	0.983	0.032	0.962	[112]
HNO3-MP		2.223	2.702703	0.972	0.034	0.962	
H2SO4-MP		2.654	2.941176	0.993	0.032	0.951	
C2H4O2-MP		1.914	2.12766	0.979	0.035	0.998	
H3PO4-MP		2.142	2.325581	0.972	0.032	0.953	
HCl-MP		1.5323	1.923077	0.961	0.038	0.991	
Modified aged refuse (MAR)	Langmuir	22.2255	0.1035	0.9534	0.0817	0.9998	[113]
Magnetic anion exchange resin (MAER-1)	Freundlich	6.886	1.494	0.9709	0.00331	0.9493	[81]
MAER-2	Freundlich	5.017	1.403	0.9834	0.00254	0.9738	
MAER-3	Freundlich	11.94	1.654	0.9875	0.00545	0.9529	
DPCS0.05	Langmuir	Not reported	Not reported	0.895	6.59	0.952	[67]
HAP/γ-Fe_2O_3	Freundlich and Sips	16.63	4.249894	0.9991	0.272	0.8614	[90]
Fe_3O_4 nanoparticles	Sips	4.16	1.785714	0.98	0.16	0.988	[50]
PANI/H-TNB	Langmuir	93.78	4.03	0.736	0.099	0.94	[97]
Ziziphus jujuba	Freundlich	9.78	2.02	0.949	0.22	0.978	[60]
MWCNTs	Freundlich	48.66	0.684932	0.91	0.0017	0.88	[66]
Eggshell powder	Freundlich	33.95	2.86	0.9996	0.108	0.895	[114]
	Langmuir	43.51	3.04	0.927	1.16	0.996	[115]
MWCNTs-Zag	Langmuir	Not reported	Not reported	Not reported	0.54159	0.92957	[77]
ZN-Ag	Langmuir	Not reported	Not reported	Not reported	0.0522	0.95646	
nZVI/chitosan	Freundlich	43.89	1.67	0.9920	0.01	0.9998	[92]
Blast furnace hydrogarnet	Freundlich	1.5	1.09	0.978	0.006	0.975	[106]

adsorption, or that adsorption occurs in a homogeneous state [119,120].

It can be observed in Table 8 that values of K_L vary drastically from 0.004 L/mg to 6.6 L/mg and there is no specific value that K_L should fall within. However, it is good to note that as the value of K_L increases, the adsorption capacity decreases, this is evident when comparing clay "Y-Na^+" which had a K_L value of 0.049 L/mg and a HA adsorption capacity of 115 mg/g, and DPCS0.05 with a K_L value of 6.59 L/mg and an adsorption capacity of 99 mg/g. The value of K_L is mainly influenced by the relationship between the surface area and porosity of the adsorbent which in turn influences the adsorption capacity [121]. Another great tool to explore the isotherms of adsorption is through the R_L value or the separation factor. Different values of R_L suggest if the adsorption process is favorable or not. Studies in this paper barely addressed R_L calculations and therefore more information is needed to report such data and discuss them.

4.1.2. Freundlich isotherm

The non-linear form of the Freundlich isotherm is given as [122]:

$$q_e = k_F\, C_e^{\left(\frac{1}{n}\right)}$$

where k_F is the Freundlich constant (mg/g) $(L/g)^n$, and n is the adsorption intensity [123].

The Freundlich isotherm assumes multi-layer adsorption and that adsorption occurs in a heterogeneous state. It can be seen in Table 8 that the value of K_F can vary drastically, however, it can be noticed that for higher values of K_F, the adsorption capacities of adsorbents are also enhanced [120], this is valid for adsorbents following the Freundlich isotherm. For instance, Hm_1 adsorbent attained a K_F value of 0.05 $(mg/g)(L/mg)^{1/n}$ and a corresponding adsorption capacity of 0.135 mg/g, while for Fe_3O_4@HPEI the K_F value of 879 $(mg/g)(L/mg)^{1/n}$ corresponds to an adsorption capacity of 476 mg/g. This suggests that the higher the Freundlich coefficient, the greater the adsorption capacity of the adsorbent. Another important parameter in isotherm studies is the adsorption intensity. When adsorption intensity "n" is >1, this suggests that adsorption is favorable. In this case, the adsorption of HA on HAP/γ-Fe_2O_3 is much more preferable than the adsorption on MWCNTs since the n values are 4.25 and 0.685 respectively. It can also be observed that greater intensity of adsorption results in greater adsorption capacity as well.

It was observed from Table 8 that the majority of the isotherm studies in the previous cases obeyed the Langmuir isotherm. This suggests that the adsorption of HA onto adsorbents usually occurs in single or homogenous layers.

4.2. Kinetic models

Kinetic models are important in the study of adsorption systems and mechanisms since it demonstrates and predicts the removal rates of pollutants. The two most common kinetic models are pseudo-first order (PFO) and pseudo-second-order kinetics (PSO). Kinetic models are

implemented by plotting the change in concentration over the change in time to be able to calculate the rate at which HA particles are removed from the solution, assuming the uptake is first-order or second order.

4.2.1. Pseudo-first order kinetic model

The non-linear form of the PFO kinetic model is shown as [116,124]:

$$q_t = q_e - q_e exp(-k_1\, t)$$

where q_t is the adsorption capacity at time = t (mg/g), t is time (s), and k_1 is the rate constant (min^{-1}).

4.2.2. Pseudo-second order kinetic model

The non-linear form of the PSO kinetic model is demonstrated as [125,126]:

$$q_t = \frac{q_e^2\, k_2 t}{1 + q_e k_2 t}$$

where k_2 is the PSO rate constant (g/mg·min).

It was observed that most of the kinetic studies were fitted as PSO, this shows that the adsorption of HA is mainly a chemical process and not a physical process. Usually, when k_2 is much greater than k_1, the adsorption process can be characterized as chemisorption [100]. Table 9 shows some reported adsorbents and the kinetic studies parameters such as pseudo-first and pseudo second-order rate constants and corresponding R^2 values. It was evident that k_2 values were mostly <1, however, there are some anomalies in the data where the value of k_2 is much >1. The value of k_2 usually depends on the operating conditions of the adsorption process such as pH, initial concentration, etc. Moreover, the value of k_2 is influenced by the particle size of the adsorbent, this means that with larger particle sizes, smaller k_2 values are expected, and this is due to an increase in interparticle diffusion resistance [127].

5. Factors affecting the adsorption process

5.1. Effect of changing pH

In most of the adsorption studies, the adsorption process was found to be heavily dependent on pH, and it was also evident from Fig. 8 that 78 % of adsorbents were best performing at lower pH (acidic region pH < 7). Unanimously, the effect of pH on the adsorption process - regardless of the adsorbent used - was that as the pH increased, the

Table 9
Kinetic data of different adsorbents discussed.

Adsorbent	Kinetic model	PFO		PSO		Reference
		k1 (min^{-1})	R^2	k2 (g mg^{-1} min^{-1})	R^2	
Fe_3O_4-Zn/Al-LDH	PSO	0.009	0.9404	444	0.9963	[98]
CA/CS nanofibers	PFO	0.05	0.98	0.19	0.95	[101]
ZnO-30N-zeolite	PSO	1.4494	0.9769	0.0743	0.9998	[79]
PANI-coated mask	PSO	0.0459	0.942	0.0166	0.999	[96]
Graphene (G)	PSO	0.03	0.39	0.16	1	[65]
Graphene oxide (GO)	PSO	0.02	0.8	0.05	1	
PCL	PSO	0.006389	0.7207	0.0153	0.9991	[49]
QCL	PSO	0.063483	0.7772	0.0229	0.9982	
$FeNi_3/SiO_2/TiO_2$	PSO	0.0175	0.81	0.00339	0.99	[89]
Fe_3O_4@HPEI	PSO	0.000036	0.42	0.0000087	0.999	[100]
Hydrogarnet/zeolite composite	PSO	Not reported	Not reported	0.00383	Not reported	[83]
CoFe2O4@PBC-LDH	PSO	1.8108	0.9475	0.0276	0.9651	[88]
CoFe2O4@BBC-LDH	PSO	1.3278	0.8651	0.0118	0.9097	
FLDH	PSO	0.013	0.7615	0.00029	0.9997	[99]
MLDH	PSO	0.004	0.9698	0.00014	0.9998	
Nano-ZIF-8	PSO	0.741473	0.997	0.0016	0.982	[84]
AC/Fe3O4@SiO2-APTMS	PSO	0.0294	0.0699	0.946	0.999	[52]
AC	PSO	0.0474	0.9099	0.0028	0.9914	[62]
AC-nZVI	PSO	0.0437	0.8266	0.0108	0.9998	
Raw pumice	PSO	0.031	0.843	0.004	0.952	[112]
HNO3-MP		0.053	0.874	0.005	0.989	
H2SO4-MP		0.034	0.967	0.004	0.945	
C2H4O2-MP		0.036	0.965	0.006	0.923	
H23PO4 - MP		0.039	0.896	0.006	0.953	
HCl-MP		0.034	0.893	0.008	0.978	
Bentonite	PSO	0.04	0.49	0.06	1	[74]
Montmorillonite		0.01	0.03	0.11	1	
Modified age refuse (MAR)	PSO	0.092	0.9187	0.002	0.9952	[113]
Magnetic anion exchange resin (MAER-1)	PSO	0.02247	0.9378	0.0007304	0.9883	[81]
MAER-2	PSO	0.01572	0.9492	0.0004582	0.9973	
MAER-3	PSO	0.02429	0.9302	0.0007197	0.9863	
DPCS0.05	PSO	0.0029	0.5492	0.00118	0.9998	[67]
HAP/γ-Fe_2O_3	PSO	0.00723	0.9461	0.00821	0.9995	[90]
Fe_3O_4 nanoparticles	PSO	0.029	0.918	0.059	0.998	[50]
ZnO coated zeolite	PSO	0.019	0.9816	0.0064	0.9966	[80]
PANI/H-TNB	PSO	0.010133	0.902	0.000326667	0.998	[97]
Ziziphus jujuba	PSO	0.00928	0.776	0.0003	0.988	[60]
Iron supported oyster shell	PSO	Not reported	Not reported	Not reported	Not reported	[91]
MWCNTs	PSO	0.016	0.51	0.026	0.99	[66]
Fe@Fe2O3 core-shell	PSO	Not reported	Not reported	Not reported	Not reported	[93]
Eggshell powder	PSO	0.05	0.749	0.113	0.999	[114]
	PSO	0.28	0.926	0.01	0.998	[115]
MWCNTs-Zag	PSO	Not reported	Not reported	0.003	0.978	[77]
ZN-Ag		Not reported	Not reported	0.026	0.9999	
ZN-Ag	PSO	Not reported	Not reported	14.336	0.99997	[78]
ZA-Ag		Not reported	Not reported	2.9574	1	
nZVI/chitosan	PSO	0.1303	0.9863	0.0001	0.9998	[92]

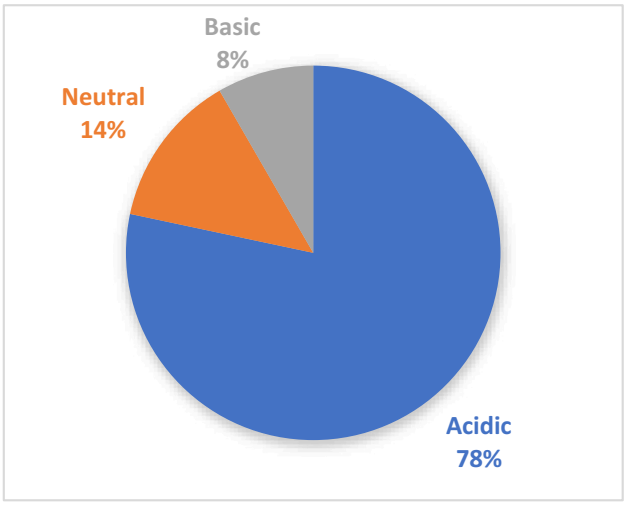

Fig. 8. Operating pH range of all adsorbents used for humic acid removal including all publications cited in the current work.

amount of HA adsorbed on the surface decreased. There were several reasons for this trend since the amount adsorbed depends on the nature of the adsorbent surface as well as the properties of HA. Although HA can exist in several and distinct structures, characterization methods confirmed the presence of carboxylate groups, aliphatic and aromatic hydroxyl groups which make HA negatively charged at high pH (pH > 2) [8].

According to Santosa et al., the increase in pH disrupts the inter and intra-bonds of hydrogen due to the ionization of the carboxyl group to a carboxyl anion, which would break up the HA structure [98]. With PANI-coated adsorbents, it was realized that the positively charged surface adsorption was enhanced due to stronger electrostatic attraction between the surface and the negatively charged HA at lower pH [96].

The value of the adsorbent's zero-point charge (ZPC) also affects the surface's charge at different pH values. Most adsorbents such as QCL, natural clay and $FeNi_3/SiO_2/TiO_2$ exhibited positive charges at lower pH, which facilitated the adsorption of the negatively charged HA [46,70,89]. Moreover, HA was found to have a higher solubility in a highly acidic medium and this property enhanced the adsorption of HA [65,88]. However, decreasing the pH and especially the extremely acidic conditions facilitate the HA precipitation to form a sludge that becomes tedious to remove and expensive to treat [96,101]. Since HA would be positively charged at low pH values, electrostatic repulsion can result if the surface charge of the adsorbent is also positive [60].

Conversely, it can be observed in some studies that the increase in pH had a considerably positive impact on the adsorption capacities of some adsorbents [60,81,85]. This behavior was reasoned by the dissociation of carboxylic and phenolic groups that are part of the HA structure [85] as well as the variation of the zeta potentials due to this dissociation [81]. The most prominent reason would be the HA and adsorbent interaction at the specific pH [60].

In other studies, such as using ZnO-30N zeolite [80] adsorbent as well as vermiculite/palygorskite [43], the pH had negligible or almost no effect on the adsorption process. This was explained by the nature of the columbic interaction between the surface of the adsorbent and the HA structure [80]. No further explanation was provided regarding this phenomenon; however, it is worth noting that the isoelectric point of the adsorbent surface may be very high and therefore any change in the pH of the solution would not affect the adsorbent surface as much as it would if the material had a lower isoelectric point or point of zero charges.

5.2. Effect of initial humic acid concentration

Adsorption is a mass transfer phenomenon, and that suggests that the movement of particles from the solution (high concentration) to the adsorbent surface (low concentration) is mainly facilitated by the concentration gradient and hence the adsorption process relies so much on the initial HA concentration [8,123]. As the initial HA concentration increases, the amount of adsorbed HA increases. This trend is justified, since increasing the initial HA concentration enhances the concentration gradient and in turn, a greater driving force [63,108] between the solution and adsorbent surface. This causes more HA molecules to be adsorbed [70,95,96] at higher concentrations and the resistive forces from liquid to adsorbent are overcome [91,100]. On the contrary, there are instances where an increase in the initial concentration of HA in the solution causes a decrease in the adsorption capacity and a decline in the performance of the adsorbent. The reason for this trend is that as the concentration of HA increases, and the dosage is kept constant, the available surface area decreases, and therefore decreasing the adsorption capacity [53,62,89,112] since there are fewer available sites for the adsorption of HA.

5.3. Effect of contact time

The contact time has an impact on the adsorption process since it is performed in batch systems. As the contact time between the adsorbent and water increases, the amount of HA adsorbed increases and once equilibrium is reached, no more HA is adsorbed. Moreover, at initial times the rate of adsorption is very fast until equilibrium times are reached, then adsorption slows down and reaches a plateau. This trend was justified by several studies, where it is explained that the pores and spaces are vacant initially, and as time passes and equilibrium times are reached, the spaces become occupied and are eventually full where no more adsorption can occur [65,89,100,101]. Moreover, this plateau can also be justified by the increase in repulsive forces amongst the adsorbed HA molecules due to electrostatic repulsion [66,108]. This trend was prevailing and unanimous amongst all the studies presented in this paper.

5.4. Effect of adsorbent dosage

The adsorbent dosage influences the adsorption process, but this varies from one adsorbent to another. In some cases, increasing the adsorbent dosage enhanced the adsorption process, such as demonstrated using Fe_3O_4@HPEI [100], PANI [95], pumice and its modified forms [112], HAP/γ-Fe_2O_3 [90], Fe_3O_4 nanoparticles [50], ZnO-30N zeolite [80] and oyster shell-nZVI [91] adsorbents. The enhancement in adsorption was due to more adsorption sites that allow for more HA to be adsorbed on the surface.

On the contrary, contrasting trends were observed for adsorbents such as CA/CS, $FeNi_3/SiO_2/TiO_2$, G, GO and MWCNTs. As the dosage of these adsorbents increased, the adsorption for HA decreased, this was justified by the unsaturation of the surface where the entire capacity of the adsorbent is not utilized [66,89] as well as the increase of interaction between HA particles which decreases the amount of HA adsorbed [65]. This trend is also observed within many other adsorbents such as AC, bentonite and montmorillonite nanoparticles and MAR. These trends and observations were justified. As the adsorbent dosage increases, competition amongst the HA molecules resulted in a lower capacity of HA removal [59] and a decrease in the driving force, due to a high number of pores and insufficient HA concentration in the solution to keep up with the adsorption process [74,113]. Moreover, agglomeration can also take place which reduces the effectiveness of the adsorbent and cause the pollutant to overlap and crowd at higher dosage [114]. On another note, the adsorbent dosage is an important operational parameter that needs to be taken into consideration since it shapes the efficacy of the adsorbent as well as determines the cost-effectiveness of the

process which is of high importance on the industrial scale.

5.5. Effect of temperature

The temperature at which the adsorption experiments are conducted plays a major role in the performance of adsorbents. The effect on the adsorption process is mainly determined through thermodynamic analysis considering the evaluation of Gibbs free energy changes. For adsorbents such as G, GO [65], nano-ZIF8 zeolite [84], and vermiculite/palygorskite composite [43], an increase in temperature will decrease the adsorption capacity or percentage removal of HA from water. This is because the adsorption process of these pollutants is an exothermic reaction. This might be justified because an increase in temperature increases the kinetic energy of the particles. This may result in frequent collisions and often a difficulty for the HA particles to stay within the pores. Contrarily, the effect of temperature can be quite the opposite, as an increase in temperature will result in an enhanced adsorption capacity and efficiency. This trend can be linked to the adsorption process being an endothermic process [8,50,52,74]. There might also be other explanations for this trend, such as in AC [59], where the increase in capacity at higher temperatures might suggest that the adsorption process is physical because of the increase in the degree of freedom at the solid-liquid interface during adsorption. When studying *Ziziphus jujuba* adsorbent, the increase in capacity with increasing temperatures is attributed to the formation of new sites as well as the speeding up of originally slower steps in adsorption [60]. It was also observed that as the temperature increased, the internal structure of the oyster shell-nZVI adsorbent swelled up, hence, enhancing the interaction between adsorbent and adsorbate. Moreover, the diffusion rate of HA into both the external and porous layers increases as temperature rises [91]. Using eggshell adsorbent [114] for the removal of HA from water, the variation of temperature did not affect HA removal or the performance of the adsorbent and was considered merely an economic aspect. This suggests that in this case, a lower temperature is preferred due to lower costs of operation (since higher temperatures require more energy and are therefore economically unfavorable).

5.6. Effect of ionic strength

The availability of anions and cations (in other words, the ionic strength), plays a role in the performance of the adsorption process and has a major effect on it. Ionic strength is usually investigated through the variation of concentrations of KNO_3, Ca $(NO_3)_2$, or even NaCl. According to Hosseinzehi et al., as the concentration of NaCl varied from 50 to 1000 mg/L, the amount of HA adsorbed on AC/Fe_3O_4@SiO_2-APTMS slightly decreased from 98 % to 95 %, which was a result of the competition between the chlorine anions and the HA functional groups [52]. In contrast, the increase of ionic strength (through the increase of concentrations of KNO_3 and Ca $(NO_3)_2$) increases the ability of HAP/γ-Fe_2O_3 and ZnO-30N zeolite adsorbents to remove HA. This was attributed to the complexation of the surface in HAP/γ-Fe_2O_3 [90], while in ZnO-30N zeolite [80], it was because of the electrostatic repulsion between the HA in the solution and HA that is adsorbed on the surface due to calcium ion bridging [128]. Therefore, it is recommended to direct research towards the effect of ionic strength on the removal of HA from water, which would benefit in coming up with solutions for HA removal in water types with very high salinity or ionic strength, and also because there could be various types of ions in the water that can affect the adsorption of HA.

6. Regeneration of adsorbents

The regeneration and reusability of adsorbents are vital considerations when assessing the effectiveness of the adsorbent because capacity alone is insufficient in determining its efficacy. Regeneration of the adsorbent involves desorption of the adsorbate (in this case HA) and going through the adsorption process again to evaluate if the adsorbent under study can be used more than once. This is useful in the industrial field because it is considered cost-effective to be able to reuse the same adsorbent instead of consuming fresh adsorbent for each cycle, especially when the adsorbent saturates in a short time. The regeneration of adsorbents could be performed chemically, and thermally, using ultrasonication or washing with water.

The most prominent method of regeneration was using chemical eluents to desorb the HA from the pores of the adsorbents such as NaOH solution. PCL and QCL adsorbents were regenerated once using 3 M NaOH for 24 h and the efficiency was reduced to 76 % for both adsorbents [49] which is a quite significant drop in efficiency for the first cycle only. Similarly, Fe_3O_4@HPEI was regenerated four times using 0.1 M NaOH, and after the 4th cycle, the efficiency of adsorption decreased by 17 % [100]. Adsorbents prepared from functionalized magnetic biochar on popular sawdust ($CoFe_2O_4$@PBC-LDH) and bamboo powder ($CoFe_2O_4$@BBC-LDH) were regenerated using 0.1 M NaOH as eluent for 2 h followed by washing with deionized water [88]. The adsorbents were able to be reused for 7 cycles, where after 7 cycles, the adsorption capacity of $CoFe_2O_4$@PBC-LDH decreased by 29 %, while for $CoFe_2O_4$@BBC-LDH the capacity decreased by 46 %. This is a major decrease; however, it can be seen that this was reasonable since 7 cycles were achieved before the capacity is compromised. AC/Fe_3O_4@SiO_2–APTMS could also be recycled using NaOH as an eluent for 4 cycles, after which the efficiency of the adsorbent decreased to approximately 65 % [52]. It can be argued that the efficiency drops drastically after 4 cycles, however, after the first cycle, the capacity is barely compromised, so a reasonable number of reuses should be established to be <4 and >1. Analogously, activated carbon with nZVI (AC-nZVI) was regenerated for 5 cycles using 0.1 M NaOH solution [62]. After 5 cycles, the efficiency has decreased by 27 % and similar to AC/Fe_3O_4@SiO_2–APTMS, after the first cycle, the efficiency dropped to 93 % which is not that significant, and therefore a suitable number of cycles is required between 1 and 5. PANI/H-TNB underwent regeneration studies using NaOH as an eluent (0.1 M) [97]. The capacity of PANI/H-TNB was reported to decrease from 129 mg/g in the first cycle to approximately 97 mg/g after the 10th cycle. This is a significant decrease even from the first cycle since the adsorption capacity reported in the study was 340 mg/g which corresponds to a >40 % drop in the first cycle only. This was justified by the deficient desorption of HA molecules from the adsorbent surface, and this calls for an optimization of the desorption process, perhaps experimenting with other desorption/regeneration methods.

Other eluents can be used for the regeneration of adsorbents, such as ethanol, HCl, NaCl solution, or even deionized water (MilliQ) that is altered at different pHs. For example, surfactant-modified zeolite (SMZ) was regenerated using 25 % (v/v) of ethanol solution for three cycles [85]. It was effective after 3 cycles, as the capacity was barely affected (approx. 4 % decrease in capacity). The regeneration of MAER-3 was compared using a NaCl solution (10 % w/w) and a mixture of NaCl and NaOH (10 %, 1 %) [81]. It was found that the pure NaCl solution was less effective than the mixture of NaCl and NaOH, since after 21 cycles the decrease in adsorption efficiency was 26 % and 7 % respectively. On another note, the regeneration of nano-ZIF-8 zeolite was attempted using water at 25 °C which was ineffective [84]. Therefore, water at 85 °C was used and was successful for 4 cycles where the efficiency was insignificantly reduced to 90 %.

Ultrasonication can also be used for the regeneration of AC [59]. The process of ultrasonication involves subjecting the liquid to high-frequency ultrasound waves with a frequency of >20 kHz to facilitate agitation. The process of ultrasonication was performed at a frequency of 37 kHz to desorb the HA from the AC for 10 min, and after the first cycle, the adsorption capacity was shown to increase to approximately 43 mg/g [59], this increase was not justified and was probably due to a change in the morphology when subjected to high amounts of energy. After the first cycle, the capacity was not affected as much and was insignificant, however, it was justified by the blockage of the pores on

the surface.

Thermal regeneration was proven effective in many adsorbents such as nano-MgO, FLDH, MLDH and Fe-montmorillonite. FLDH and MLDH underwent thermal treatment at 455 °C for 6 h and then used 0.03 M of KNO_3 [99]. Both of the adsorbents were able to achieve <20 % capacity reduction after 5 cycles which was a great performance. Moreover, Fe-montmorillonite was regenerated by calcination at 300 °C and was able to achieve 5 cycles of regeneration without compromising adsorption efficiency [53]. Also, nano-MgO was regenerated by annealing (type of heat treatment) at 500 °C for 10 cycles and even after 10 cycles, the adsorption capacity barely decreased [107]. This shows thermal regeneration is an effective form of regeneration that ensures the integrity of the adsorbent and that does not compromise the adsorption capacity. Nevertheless, it needs to be taken into consideration that heat treatment at very high temperature such as discussed previously are not environmentally friendly since they require an energy source and ultimately its cost is increased due to the need for constant heating for regeneration.

The adsorbent that was able to achieve the best regeneration ability (despite the adsorption capacity) was MAER-3, with 21 cycles and where the capacity was not drastically compromised. This is attributed to its high DAI content, which also contributed to anti-fouling properties.

7. Conclusions and recommendations

In conclusion, humic acid is a type of natural organic matter that is formed from the decomposition of organic matter and is a critical pollutant to remove. Humic acid can react with disinfectants to produce carcinogens and toxic substances, and the need for its removal is critical. Adsorption is an effective process for the removal of humic acid from wastewater as many types of adsorbents were able to efficiently remove HA such as AC/carbon-based, zeolites/resins, natural and modified clays, iron-based, PANI-based, functionalized, and natural adsorbents.

Adsorption of HA is dependent on many factors such as pH, initial HA concentration, adsorbent dosage and contact time. The adsorption of HA on many adsorbents mostly followed the Langmuir isotherm and was characterized by pseudo-second-order kinetics. When comparing the adsorbents, the adsorbent with the greatest reusability was MAER-3 with 21 cycles of regeneration. On the other hand, nano-MgO achieved the best HA adsorption capacity of 1260 mg/, and garnet achieved the lowest adsorption capacity of 0.001 mg/g. However, the adsorbent that achieved the best performance in terms of both regeneration and capacity was nano-MgO, where 10 regeneration cycles were achieved, and the efficiency stayed above 99 % even after 10 cycles. However, the main drawback of reusing nano-MgO was that the regeneration was at a high temperature of 500 °C, which is not cost-effective or environmentally friendly. It can be concluded that the functionalized adsorbents had the best performance since most of them could achieve high capacities of HA adsorption as well as regeneration abilities.

When reviewing the literature, it was evident that the focus was mainly on studying adsorption in batch processes. Therefore, more effort should be driven towards studying continuous adsorption processes such as the use of fixed-bed processes. Moreover, studies were focused on evaluating the removal of humic acid from synthesized solutions, new studies should utilize actual wastewater from effluents of treatment plants as part of their analyses to attain more realistic and relatable numbers for adsorption capacities and operational parameters. To implement these treatment processes, cost analysis should be carried out to assess the feasibility of the treatment process, as well as the comparison between the adsorbents when implementing them on an industrial scale. Another promising approach is the use of integrated processes for wastewater treatment, the applications for this idea can be further applied and utilized in the removal of humic acid from wastewater. Leaching of ionic compounds such as iron from the adsorbent surface is also a possible phenomenon that can occur if the adsorbent is unstable. This could suggest that the treated water is contaminated as well as the adsorbent surface and adsorption performance is compromised. No information regarding this phenomenon was discussed in the available literature, and therefore it would be beneficial to investigate this issue even further.

Abbreviations

HA	Humic acid
DOC	Dissolved organic carbon
DBP	Disinfection by-product
IARC	International Agency for Research on Cancer
AOP	Advanced oxidation process
AC	Activated carbon
Cm1	Cullar D
Hm1	Hydraffin 30 N
G	Graphene
GO	Graphene oxide
ZIF-8	Zeolitic Imidazolate Framework – 8
PANI	Polyaniline
LDH	Layered double hydroxides
FLDH	Flake Zn-Al LDH
MLDH	Microsphere LDH
HPEI	Hyper balanced polyethyleimine
$CoFe_2O_4$@PBC-LDH	Mg/Al-LDH with magnetic biochar on poplar sawdust
$CoFe_2O_4$@BBC-LDH	Mg/Al-LDH with magnetic biochar on bamboo powder
CA	Cellulose acetate
CS	Chitosan fibers
DMAEMA	Dimethyl aminoethyl methacrylate
QCL	Quaterinized DMAEMA on cotton-linter
PCL	Protonated DMAEMA on cotton-linter
PFO	Pseudo-first order
PSO	Pseudo-second order
nZVI	Nano zero valent iron
MWCNT	Multiwalled carbon nanotubes
DPCS	Dual-pore mesoporous carbon shell
KTD-Kaolinite	Kaolinite extracted from King Talal sediments
FHA-Kaolinite	Commercially bought kaolinite
Fe-Montmorillonite	Iron modified montmorillonite
ZN-Ag	Natural silver doped zeolite
MWCNT-Z Ag	Multiwalled carbon nanotubes silver doped natural zeolite
ZA-Ag	Synthetic silver doped natural zeolite
ZnO-30N zeolite	ZnO coated zeolite modified with 30 % nitric acid
MAER	Magnetic anion exchange resin
DAI	Diallyl itaconate
NZ	Natural zeolite
SMZ	Surfactant modified zeolite
HDMTA	Hexadecyltrimethylammonium bromide
AC/Fe_3O_4@SiO_2–APTMS	AC from sawdust, magnetized by Fe_3O_4, coated by SiO_2 and functionalized by APTMS
APTMS	3-Aminopropyltrimethoxysilane
HAP/γ-Fe_2O_3	Maghemite incorporated hydroxyapatite
Fe_3O_4–NP	Magnetic nanoparticles
Fe@Fe_2O_3	Core shell nanowires
PANI/H-TNB	Polyaniline/hydrogen-titanate nanobelt composite
NOM	Natural organic matter
MAR	Modified aged refuse
$C_2H_2O_2$–MP	Pumice stone modified with acetic acid
HCl–MP	Pumice stone modified with hydrochloric acid
HNO_3–MP	Pumice stone modified with nitric acid
H_2SO_4–MP	Pumice stone modified with sulfuric acid
Fe_3O_4	Magnetite
Fe_3O_4–Zn/Al LDH	Composite of magnetite and Zn-Al LDH
Fe_3O_4@HPEI	Magnetite modified with HPEI

ppAA	Plasma polymerized allylamine
CEC	Cation exchange capacity
CNS	Central nervous system

Declaration of competing interest

The authors declare that they have no known competing financial interests or personal relationships that could have appeared to influence the work reported in this paper.

Data availability

Data will be made available on request.

Acknowledgment

This publication was supported by Qatar University internal grant (QUCG-CENG-23/24-111). The findings achieved herein are solely the responsibility of the authors. Open Access funding is provided by the Qatar National Library.

References

[1] X.-W. Tan, X.-L. Zhou, R. Hua, Y.-Y. Zhang, Technologies for the removal of humic acid from water: a short review of recent developments, in: 2010 4th Int. Conf. Bioinforma. Biomed. Eng, IEEE, 2010, https://doi.org/10.1109/ICBBE.2010.5518283.
[2] A. Sharifi, A.R. Abhari, S. Farrokhzadeh, Z. Mahmoodi, N. Sadeghi, Application of cr-doped ZnO for photocatalytic degradation of organic pollutants from aqueous solutions, Int. J. Environ. Sci. Technol. (2021), https://doi.org/10.1007/s13762-021-03290-6.
[3] M. Inyang, E. Dickenson, The potential role of biochar in the removal of organic and microbial contaminants from potable and reuse water: a review, Chemosphere 134 (2015) 232–240, https://doi.org/10.1016/j.chemosphere.2015.03.072.
[4] S. Basumallick, S. Santra, Monitoring of ppm level humic acid in surface water using ZnO–chitosan nano-composite as fluorescence probe, Appl Water Sci 7 (2017) 1025–1031, https://doi.org/10.1007/s13201-015-0291-1.
[5] D. Kulikowska, B.K. Klik, Z.M. Gusiatin, K. Hajdukiewicz, Characteristics of humic substances from municipal sewage sludge: a case study, Desalin. Water Treat. 144 (2019) 57–64, https://doi.org/10.5004/dwt.2019.23622.
[6] M. Mohsin, I.A. Bhatti, A. Ashar, M.W. Khan, M.U. Farooq, H. Khan, M. T. Hussain, S. Loomba, M. Mohiuddin, A. Zavabeti, M. Ahmad, M. Yousaf, N. Mahmood, Iron-doped zinc oxide for photocatalyzed degradation of humic acid from municipal wastewater, Appl. Mater. Today 23 (2021), 101047, https://doi.org/10.1016/j.apmt.2021.101047.
[7] A.M.K. Pandian, M. Rajamehala, M.V.P. Singh, G. Sarojini, N. Rajamohan, Potential risks and approaches to reduce the toxicity of disinfection by-product – a review, Sci. Total Environ. 822 (2022), https://doi.org/10.1016/j.scitotenv.2022.153323.
[8] A. Burilo, M. Šiljeg, M. Ergović Ravančić, A. Pala, M. Pagaimo, V. Teixeira, S. Paixão, A. Zeko-Pivač, D. Kukić Grgić, A. Tutić, M. Habuda-Stanić, Adsorption of humic acid from water using chemically modified bituminous coal-based activated carbons, Chem. Biochem. Eng. Q. 35 (2021) 189–203, https://doi.org/10.15255/CABEQ.2021.1933.
[9] M.S. Algamdi, I.H. Alsohaimi, J. Lawler, H.M. Ali, A.M. Aldawsari, H.M. A. Hassan, Fabrication of graphene oxide incorporated polyethersulfone hybrid ultrafiltration membranes for humic acid removal, Sep. Purif. Technol. 223 (2019) 17–23, https://doi.org/10.1016/j.seppur.2019.04.057.
[10] Y. Yue, G. An, L. Liu, L. Lin, R. Jiao, D. Wang, Pre-aggregation of Al13 in optimizing coagulation for removal of humic acid, Chemosphere 277 (2021), 130268, https://doi.org/10.1016/j.chemosphere.2021.130268.
[11] D.C.A. Gowland, N. Robertson, E. Chatzisymeon, Photocatalytic oxidation of natural organic matter in water, Water 13 (2021) 288, https://doi.org/10.3390/w13030288.
[12] J. Ryu, J. Jung, K. Park, W. Song, B. Choi, J. Kweon, Humic acid removal and microbial community function in membrane bioreactor, J. Hazard. Mater. 417 (2021), https://doi.org/10.1016/j.jhazmat.2021.126088.
[13] V. Shankar, J. Heo, Y. Al-Hamadani, C. Park, K. Chu, Y. Yoon, Evaluation of biochar-ultrafiltration membrane processes for humic acid removal under various hydrodynamic, pH, ionic strength, and pressure conditions, J. Environ. Manage. 197 (2017) 610–618, https://doi.org/10.1016/j.jenvman.2017.04.040.
[14] M.A. Islam, D.W. Morton, B.B. Johnson, M.J. Angove, Adsorption of humic and fulvic acids onto a range of adsorbents in aqueous systems, and their effect on the adsorption of other species: a review, Sep. Purif. Technol. 247 (2020), 116949, https://doi.org/10.1016/j.seppur.2020.116949.
[15] W.-W. Tang, G.-M. Zeng, J.-L. Gong, J. Liang, P. Xu, C. Zhang, B.-B. Huang, Impact of humic/fulvic acid on the removal of heavy metals from aqueous solutions using nanomaterials: a review, Sci. Total Environ. 468–469 (2014) 1014–1027, https://doi.org/10.1016/j.scitotenv.2013.09.044.
[16] A. Bhatnagar, M. Sillanpää, Removal of natural organic matter (NOM) and its constituents from water by adsorption – a review, Chemosphere 166 (2017) 497–510, https://doi.org/10.1016/j.chemosphere.2016.09.098.
[17] Z. Wang, R. Bai, Y.P. Ting, Conversion of waste polystyrene into porous and functionalized adsorbent and its application in humic acid removal, Ind. Eng. Chem. Res. 47 (2008) 1861–1867, https://doi.org/10.1021/ie070583m.
[18] Y.S.S. Al-Faiyz, CPMAS 13 C NMR characterization of humic acids from composted agricultural saudi waste, Arab. J. Chem. 10 (2013), https://doi.org/10.1016/j.arabjc.2012.12.018.
[19] C. Steelink, What is humic acid? J. Chem. Educ. 40 (1963) 379, https://doi.org/10.1021/ed040p379.
[20] A. Barhoumi, S. Ncib, A. Chibani, K. Brahmi, W. Bouguerra, E. Elaloui, High-rate humic acid removal from cellulose and paper industry wastewater by combining electrocoagulation process with adsorption onto granular activated carbon, Ind. Crop. Prod. 140 (2019), 111715, https://doi.org/10.1016/j.indcrop.2019.111715.
[21] H. Rigane, M. Chtourou, I. Ben Mahmoud, K. Medhioub, E. Ammar, Polyphenolic compounds progress during olive mill wastewater sludge and poultry manure co-composting, and humic substances building (Southeastern Tunisia), Waste Manag. Res. J. Sustain. Circ. Econ. 33 (2015) 73–80, https://doi.org/10.1177/0734242X14559594.
[22] M. Zahmatkesh, H. Spanjers, J.B. van Lier, Fungal treatment of humic-rich industrial wastewater: application of white rot fungi in remediation of food-processing wastewater, Environ. Technol. 38 (2017) 2752–2762, https://doi.org/10.1080/09593330.2016.1276969.
[23] Y. Cheng, K. Chon, X. Ren, Y. Kou, M.-H. Hwang, K.-J. Chae, Bioaugmentation treatment of a novel microbial consortium for degradation of organic pollutants in tannery wastewater under a full-scale oxic process, Biochem. Eng. J. 175 (2021), 108131, https://doi.org/10.1016/j.bej.2021.108131.
[24] A. Islam, G. Sun, W. Shang, X. Zheng, P. Li, M. Yang, Y. Zhang, Separation and characterization of refractory colored dissolved effluent organic matter in a full-scale industrial park wastewater treatment plant, Environ. Sci. Pollut. Res. 28 (2021) 42387–42400, https://doi.org/10.1007/s11356-021-13732-w.
[25] Y.-M. Yoon, Y.S. Ok, D.Y. Kim, J.-G. Kim, Agricultural recycling of the by-product concentrate of livestock wastewater treatment plant processed with VSEP RO and bio-ceramic SBR, Water Sci. Technol. 49 (2004) 405–412, https://doi.org/10.2166/wst.2004.0781.
[26] M.E. Silva, M. Santos, I. Brás, Characterization of wastewater from landfills - amount and type of humic substances extracted from leachate, E3S Web Conf. 80 (2019) 03002, https://doi.org/10.1051/e3sconf/20198003002.
[27] A.M. Anielak, A. Kłeczek, Humus acids in the digested sludge and their properties, Materials (Basel) 15 (2022) 1475, https://doi.org/10.3390/ma15041475.
[28] K. Liu, Y. Chen, N. Xiao, X. Zheng, M. Li, Effect of humic acids with different characteristics on fermentative short-chain fatty acids production from waste activated sludge, Environ. Sci. Technol. 49 (2015) 4929–4936, https://doi.org/10.1021/acs.est.5b00200.
[29] R.-Q. Wang, L. Gutierrez, N.S. Choon, J.-P. Croué, Hydrophilic interaction liquid chromatography method for measuring the composition of aquatic humic substances, Anal. Chim. Acta 853 (2015) 608–616, https://doi.org/10.1016/j.aca.2014.09.026.
[30] P. Boguta, Z. Sokolowska, Interactions of Humic Acid With Metals, Institute of Agrophysics Bohdan Dobrzański PAN, Publishing House, Lublin, 2013.
[31] B.A.G. de Melo, F.L. Motta, M.H.A. Santana, Humic acids: structural properties and multiple functionalities for novel technological developments, Mater. Sci. Eng. C. 62 (2016) 967–974, https://doi.org/10.1016/j.msec.2015.12.001.
[32] R.E. Pettit, Organic matter, humus, humate, humic acid, fulvic acid and humin: their importance in soil fertility and plant health, CTI Res. 10 (2004) 1–7.
[33] S. Bhoopal Reddy, M.S. Nagaraja, G.G. Kadalli, B.V. Champa, Fourier transform infrared (FTIR) spectroscopy of soil humic and fulvic acids extracted from Paddy land use system, Int. J. Curr. Microbiol. Appl. Sci. 7 (2018) 834–837, https://doi.org/10.20546/ijcmas.2018.705.102.
[34] Merck, IR spectrum table & chart. https://www.sigmaaldrich.com/QA/en/technical-documents/technical-article/analytical-chemistry/photometry-and-reflectometry/ir-spectrum-table, 2022.
[35] M.Y. Ashfaq, M.A. Al-Ghouti, H. Qiblawey, N. Zouari, Evaluating the effect of antiscalants on membrane biofouling using FTIR and multivariate analysis, Biofouling 35 (2019) 1–14, https://doi.org/10.1080/08927014.2018.1557637.
[36] H. Schulten, M. Schnitzer, A state-of-the-art structural concept for humic substances, Naturwissenschaften 80 (1993) 29–30.
[37] W. Flaig, Chemie der humusstoffe, Acta Chem. Fenn. A. 33 (1960) 229–251.
[38] C. Steelink, Implications of elemental characteristics of humic substances, in: G. Aiken, D.M. McKnight, R.L. Wershaw, P. MacCarthy (Eds.), Humic Subst. Soil, Sediment Water Geochemistry, Isol. Charact, Wiley Interscience Publication, New York, 1985, pp. 457–476.
[39] F.J. Stevenson, Humus Chemistry: Genesis, Composition, Reactions, John Wiley & Sons, London, 1994.
[40] K. Thorn, D. Folan, P. MacCarthy, Characterization of the International Humic Substances Society Standard and Reference Fulvic and Humic Acids by Solution State Carbon-13 (13C) and Hydrogen-1 (1H) Nuclear Magnetic Resonance Spectrometry, 1989, https://doi.org/10.3133/wri894196.
[41] M. Kononowa, Organic Matter in the Soils; Its Structure, Properties, and Methods of Study, PWRL, Warsaw, Pol, 1968.
[42] Y. Siddiqu, S. Meon, R. Ismail, M. Rahmani, A. Ali, In vitro fungicidal activity of humic acid fraction from oil palm compost, Int. J. Agric. Biol. 11 (2009) 448–452.

[43] X. Zhang, G. Lv, L. Liao, M. He, Z. Li, M. Wang, Removal of low concentrations of ammonium and humic acid from simulated groundwater by vermiculite/palygorskite mixture, Water Environ. Res. 84 (2012) 682–688, https://doi.org/10.2175/106143012X13373550426751.
[44] R. Zbytniewsk, T. Kowalkowsk, B. Buszewsk, Application of mathematical and chemometrical approaches in the study of heavy metal ions – soil interactions, New Horiz. 23 (2003) 465–485. Chapitre.
[45] C. Li, S. Zhao, X. Huang, D. Xie, X. Li, J. Ma, Y. Liao, Development of humic acid based adsorbents for fast and efficient removal of ammonia and organic nitrogen from super magnetic separation treated wastewater, J. Environ. Chem. Eng. 10 (2022), 107223, https://doi.org/10.1016/j.jece.2022.107223.
[46] R.Kumar Gautam, D. Navaratna, S. Muthukumaran, A. Singh, N.More Islamuddin, Humic substances: its toxicology, chemistry and biology associated with soil, plants and environment, in: Humic Subst. [Working Title], IntechOpen, 2021, https://doi.org/10.5772/intechopen.98518.
[47] M. Schnitzer, S.U. Khan, Humic Substances in the Environment, Marcel Dekker, New York, 1972.
[48] R. Swift, Molecular weight, size, shape, and charge characteristics of humic substances: some basic considerations, in: Humic Subst. II Search Struct, 1989, pp. 449–466.
[49] J. Du, Z. Dong, Y. Pi, X. Yang, L. Zhao, Fabrication of cotton linter-based adsorbents by radiation grafting polymerization for humic acid removal from aqueous solution, Polymers (Basel) 11 (2019) 962, https://doi.org/10.3390/polym11060962.
[50] M.A. Zulfikar, F.I. Suri, H.Setiyanto Rusnadi, N. Mufti, M. Ledyastuti, D. Wahyuningrum, Fe 3 O 4 nano-particles prepared by co-precipitation method using local sands as a raw material and their application for humic acid removal, Int. J. Environ. Stud. 73 (2016) 79–94, https://doi.org/10.1080/00207233.2015.1108600.
[51] S.C.B. Myneni, J.T. Brown, G.A. Martinez, W. Meyer-Ilse, Imaging of humic substance macromolecular structures in water and soils, Science (80-.) 286 (1999) 1335–1337, https://doi.org/10.1126/science.286.5443.1335.
[52] M. Hosseinzehi, M.H. Ehrampoush, F. Tamaddon, M. Mokhtari, A. Dalvand, Eco-environmental preparation of magnetic activated carbon modified with 3-aminopropyltrimethoxysilane (APTMS) from sawdust waste as a novel efficient adsorbent for humic acid removal: characterisation, modelling, optimisation and equilibrium studies, Int. J. Environ. Anal. Chem. (2021) 1–21, https://doi.org/10.1080/03067319.2021.1928096.
[53] G. Heikal, A comparison between kaolin, montmorillonite fe-modified montmorillonite as candidate of upflow column media filter for humic acid removal from SSAS, Pol. J. Environ. Stud. 30 (2021) 2553–2560, https://doi.org/10.15244/pjoes/130131.
[54] A. Alkhouzaam, H. Qiblawey, Synergetic effects of dodecylamine-functionalized graphene oxide nanoparticles on antifouling and antibacterial properties of polysulfone ultrafiltration membranes, J. Water Process Eng. 42 (2021), 102120, https://doi.org/10.1016/j.jwpe.2021.102120.
[55] A. Alkhouzaam, H. Qiblawey, Novel polysulfone ultrafiltration membranes incorporating polydopamine functionalized graphene oxide with enhanced flux and fouling resistance, J. Membr. Sci. 620 (2021), 118900, https://doi.org/10.1016/j.memsci.2020.118900.
[56] M.-L. Cheng, H.-Y. Ho, D.T.-Y. Chiu, F.-J. Lu, Humic acid–mediated oxidative damages to human erythrocytes, Free Radic. Biol. Med. 27 (1999) 470–477, https://doi.org/10.1016/S0891-5849(99)00072-6.
[57] N.A. Atiyah, T.M. Albayati, M.A. Atiya, Functionalization of mesoporous MCM-41 for the delivery of curcumin as an anti-inflammatory therapy, Adv. Powder Technol. 33 (2022), 103417, https://doi.org/10.1016/j.apt.2021.103417.
[58] C. Johnson, Advances in pretreatment and clarification technologies, in: Compr. Water Qual. Purif, Elsevier, 2014, pp. 60–74, https://doi.org/10.1016/B978-0-12-382182-9.00029-3.
[59] A. Naghizadeh, F. Momeni, H. Kamani, Study of ultrasonic regeneration and adsorption of humic acid on activated carbon, Heal. Scope. 7 (2018), https://doi.org/10.5812/jhealthscope.80338.
[60] H.D. Bouras, O. Benturki, N. Bouras, M. Attou, A. Donnot, A. Merlin, F. Addoun, M.D. Holtz, The use of an agricultural waste material from Ziziphus jujuba as a novel adsorbent for humic acid removal from aqueous solutions, J. Mol. Liq. 211 (2015) 1039–1046, https://doi.org/10.1016/j.molliq.2015.08.028.
[61] Y. Chen, Y. Qian, J. Ma, M. Mao, L. Qian, D. An, New insights into the cooperative adsorption behavior of Cr(VI) and humic acid in water by powdered activated carbon, Sci. Total Environ. 817 (2022), 153081, https://doi.org/10.1016/j.scitotenv.2022.153081.
[62] Y. Rashtbari, H. Arfaeinia, S. Ahmadi, F. Bahrami Asl, S. Afshin, Y. Poureshgh, M. Fazlzadeh, Potential of using green adsorbent of humic acid removal from aqueous solutions: equilibrium, kinetics, thermodynamic and regeneration studies, Int. J. Environ. Anal. Chem. (2020) 1–18, https://doi.org/10.1080/03067319.2020.1796993.
[63] H. Godini, G.S. Khorramabady, S.H. Mirhosseini, The application of iron-coated activated carbon in humic acid removal from water, in: 2nd Int. Conf. Environ. Sci. Technol, IACSIT Press, 2011, pp. 32–36.
[64] A. Alkhouzaam, H. Qiblawey, M. Khraisheh, M. Atieh, M. Al-Ghouti, Synthesis of graphene oxides particle of high oxidation degree using a modified hummers method, Ceram. Int. 46 (2020) 23997–24007, https://doi.org/10.1016/j.ceramint.2020.06.177.
[65] A. Naghizadeh, F. Momeni, E. Derakhshani, M. Kamranifar, Humic acid removal efficiency from aqueous solutions using graphene and graphene oxide nanoparticles, Desalin. Water Treat. 100 (2017) 116–125, https://doi.org/10.5004/dwt.2017.21793.
[66] S.P. Moussavi, M.H. Ehrampoush, A.H. Mahvi, S. Rahimi, M. Ahmadian, Efficiency of multi-walled carbon nanotubes in adsorbing humic acid from aqueous solutions, Asian J. Chem. 26 (2014) 821–826, https://doi.org/10.14233/ajchem.2014.15609.
[67] H. Yu, Q. Zhang, M. Dahl, J.B. Joo, X. Wang, L. Wang, Y. Yin, Dual-pore carbon shells for efficient removal of humic acid from water, Chem. Eur. J. 23 (2017) 16249–16256, https://doi.org/10.1002/chem.201702318.
[68] A. Awasthi, P. Jadhao, K. Kumari, Clay nano-adsorbent: structures, applications and mechanism for water treatment, SN Appl. Sci. 1 (2019) 1076, https://doi.org/10.1007/s42452-019-0858-9.
[69] S.M.R. Shaikh, M.S. Nasser, M. Magzoub, A. Benamor, I.A. Hussein, M.H. El-Naas, H. Qiblawey, Effect of electrolytes on electrokinetics and flocculation behavior of bentonite-polyacrylamide dispersions, Appl. Clay Sci. 158 (2018) 46–54, https://doi.org/10.1016/j.clay.2018.03.017.
[70] S. Gueu, G. Finqueneisel, T. Zimny, D. Bartier, B.K. Yao, Physicochemical characterization of three natural clays used as adsorbent for the humic acid removal from aqueous solution, Adsorpt. Sci. Technol. 37 (2019) 77–94, https://doi.org/10.1177/0263617418811469.
[71] D. Bougeard, K.S. Smirnov, E. Geidel, Vibrational spectra and structure of kaolinite: a computer simulation study, J. Phys. Chem. B 104 (2000) 9210–9217, https://doi.org/10.1021/jp0013255.
[72] K. Al-Essa, Adsorption of humic acid onto jordanian kaolinite clay: effects of humic acid concentration, pH, and temperature, Sci. J. Chem. 6 (2018) 1, https://doi.org/10.11648/j.sjc.20180601.11.
[73] National Center for Biotechnology Information, PubChem Compound Summary for CID 71586775, Montmorillonite, 2022.
[74] E. Derakhshani, A. Naghizadeh, Optimization of humic acid removal by adsorption onto bentonite and montmorillonite nanoparticles, J. Mol. Liq. 259 (2018) 76–81, https://doi.org/10.1016/j.molliq.2018.03.014.
[75] X. Zou, Z. Wang, H. Ling, Optimized preparation of directional modified attapulgite and its application to adsorbance of humic acid in polluted raw water effluent, J. Residuals Sci. Technol. 13 (2016) 9–14, https://doi.org/10.12783/issn.1544-8053/13/1/2.
[76] A.F. Ali, S.M. Atwa, E.M. El-Giar, Development of magnetic nanoparticles for fluoride and organic matter removal from drinking water, in: Water Purif, Elsevier, 2017, pp. 209–262, https://doi.org/10.1016/B978-0-12-804300-4.00006-X.
[77] C. Orha, A. Pop, V. Tiponut, F. Manea, Composite material based on SILVER-doped zeolite and multi-wall carbon nanotubes for humic acid removaL, Environ. Eng. Manag. J. 12 (2013) 917–921, https://doi.org/10.30638/eemj.2013.113.
[78] C. Orha, A. Pop, C. Lazau, I. Grozescu, V. Tiponut, F. Manea, Silver doped natural and synthetic zeolites for removal of humic acid from wateR, Environ. Eng. Manag. J. 11 (2012) 641–649, https://doi.org/10.30638/eemj.2012.081.
[79] L. Wang, D.D. Dionysiou, J. Lin, Y. Huang, X. Xie, Removal of humic acid and Cr (VI) from water using ZnO–30N-zeolite, Chemosphere 279 (2021), 130491, https://doi.org/10.1016/j.chemosphere.2021.130491.
[80] L. Wang, C. Han, M.N. Nadagouda, D.D. Dionysiou, An innovative zinc oxide-coated zeolite adsorbent for removal of humic acid, J. Hazard. Mater. 313 (2016) 283–290, https://doi.org/10.1016/j.jhazmat.2016.03.070.
[81] Q. Li, J. Wu, M. Hua, G. Zhang, W. Li, C. Shuang, A. Li, Preparation of permanent magnetic resin crosslinking by diallyl itaconate and its adsorptive and anti-fouling behaviors for humic acid removal, Sci. Rep. 7 (2017) 17103, https://doi.org/10.1038/s41598-017-17360-8.
[82] National Center for Biotechnology Information, PubChem compound summary for CID 90472028, humic acid. https://pubchem.ncbi.nlm.nih.gov/compound/Humic-acid, 2022. (Accessed 8 July 2022).
[83] H. Maeda, K. Suzumura, T. Kasuga, Removal of humic acid from aqueous solutions by a novel hydrogarnet/zeolite composite, SN Appl. Sci. 2 (2020) 1763, https://doi.org/10.1007/s42452-020-03590-5.
[84] S.S.K. Jampa, A.P. Unnarkat, R. Vanshpati, S. Pandian, M.K. Sinha, S. Dharaskar, Adsorption and recyclability aspects of humic acid using nano-ZIF-8 adsorbent, Environ. Technol. Innov. 19 (2020), 100927, https://doi.org/10.1016/j.eti.2020.100927.
[85] A.F. Elsheikh, U.K. Ahmad, Z. Ramli, Investigations on humic acid removal from water using surfactant-modified zeolite as adsorbent in a fixed-bed reactor, Appl Water Sci 7 (2017) 2843–2856, https://doi.org/10.1007/s13201-016-0521-1.
[86] D. Ewis, A. Benamor, M.M. Ba-Abbad, M. Nasser, M. El-Naas, H. Qiblawey, Removal of oil content from oil-water emulsions using iron Oxide/Bentonite Nano adsorbents, J. Water Process Eng. 38 (2020), 101583, https://doi.org/10.1016/j.jwpe.2020.101583.
[87] S.T. Kadhum, G.Y. Alkindi, T.M. Albayati, Remediation of phenolic wastewater implementing nano zerovalent iron as a granular third electrode in an electrochemical reactor, Int. J. Environ. Sci. Technol. 19 (2022) 1383–1392, https://doi.org/10.1007/s13762-021-03205-5.
[88] J. Zhang, W. Lu, S. Zhan, J. Qiu, X. Wang, Z. Wu, H. Li, Z. Qiu, H. Peng, Adsorption and mechanistic study for humic acid removal by magnetic biochar derived from forestry wastes functionalized with Mg/Al-LDH, Sep. Purif. Technol. 276 (2021), 119296, https://doi.org/10.1016/j.seppur.2021.119296.
[89] F. Akbari, M. Khodadadi, A. Hossein Panahi, A. Naghizadeh, Synthesis and characteristics of a novel FeNi3/SiO2/TiO2 magnetic nanocomposites and its application in adsorption of humic acid from simulated wastewater: study of isotherms and kinetics, Environ. Sci. Pollut. Res. 26 (2019) 32385–32396, https://doi.org/10.1007/s11356-019-06371-9.
[90] M. Shi, L. Yang, Z. Wei, W. Zhong, S. Li, J. Cui, W. Wei, Humic acid removal by combining the magnetic property of maghemite with the adsorption property of

nanosized hydroxyapatite, J. Dispers. Sci. Technol. 37 (2016) 1724–1737, https://doi.org/10.1080/01932691.2016.1139462.
[91] V. Alipour, S. Nasseri, R. Nabizadeh Nodehi, A.H. Mahvi, A. Rashidi, Preparation and application of oyster shell supported zero valent nano scale iron for removal of natural organic matter from aqueous solutions, J. Environ. Heal. Sci. Eng. 12 (2014) 146, https://doi.org/10.1186/s40201-014-0146-y.
[92] N.Z. Pourbaghaei, M. Anbia, F. Rahimi, Fabrication of Nano zero valent Iron/Biopolymer composite with antibacterial properties for simultaneous removal of nitrate and humic acid: kinetics and isotherm studies, J. Polym. Environ. 30 (2022) 907–924, https://doi.org/10.1007/s10924-021-02209-z.
[93] H. Wu, Z. Ai, L. Zhang, Anoxic and oxic removal of humic acids with Fe@Fe2O3 core–shell nanowires: a comparative study, Water Res. 52 (2014) 92–100, https://doi.org/10.1016/j.watres.2013.12.041.
[94] M. Beygisangchin, S. Abdul Rashid, S. Shafie, A.R. Sadrolhosseini, H.N. Lim, Preparations, properties, and applications of polyaniline and polyaniline thin films—areview, Polymers (Basel) 13 (2021) 2003, https://doi.org/10.3390/polym13122003.
[95] S.P. Yeap, L.A.S. Thaanby, Y.C. Low, K.-W. Kow, Synthesis of polyaniline for water remediation and evaluating its feasibility to be reused as electrical conductor, Int. J. Nanoelectron. Mater. 13 (2020) 35–46.
[96] J.M.S. Goh, F. Wang, S.P. Yeap, Surface modification of recycled fabric materials with conductive polyaniline and its role in organic matter adsorption, Int. J. Environ. Sci. Technol. (2021), https://doi.org/10.1007/s13762-021-03757-6.
[97] T. Wen, Q. Fan, X. Tan, Y. Chen, C. Chen, A. Xu, X. Wang, A core–shell structure of polyaniline coated protonic titanate nanobelt composites for both Cr(vi) and humic acid removal, Polym. Chem. 7 (2016) 785–794, https://doi.org/10.1039/C5PY01721A.
[98] S.J. Santosa, P.A. Krisbiantoro, T.T. Minh Ha, N.T. Thanh Phuong, G. Gusrizal, Composite of magnetite and Zn/Al layered double hydroxide as a magnetically separable adsorbent for effective removal of humic acid, Colloids Surf. A Physicochem. Eng. Asp. 614 (2021), 126159, https://doi.org/10.1016/j.colsurfa.2021.126159.
[99] H. Khoshalhan Davoudli, S. Saadat, M. Rahsepar, F. Azadi, Investigating the role of the morphology of the zn-Al LDH on the adsorption of humic acid from aqueous solutions, Water Sci. Technol. 84 (2021) 1663–1677, https://doi.org/10.2166/wst.2021.373.
[100] S.M. Pormazar, M.H. Ehrampoush, M.T. Ghaneian, M. Khoobi, P. Talebi, A. Dalvand, Application of amine-functioned Fe3O4 nanoparticles with HPEI for effective humic acid removal from aqueous solution: modeling and optimization, Korean J. Chem. Eng. 37 (2020) 93–104, https://doi.org/10.1007/s11814-019-0411-y.
[101] Y. Zhang, F. Wang, Y. Wang, Electrospun cellulose acetate/chitosan fibers for humic acid removal: construction guided by intermolecular interaction study, ACS Appl. Polym. Mater. 3 (2021) 5022–5029, https://doi.org/10.1021/acsapm.1c00778.
[102] Y. Zhang, Y. Wang, Electrospun cellulose-acetate/chitosan fibers for humic-acid removal: improved efficiency and robustness with a Core-sheath design, Nanomaterials 12 (2022) 1284, https://doi.org/10.3390/nano12081284.
[103] W. Huifang, Y. Lingzhi, W. Zhiyuan, H. Jiang, C. Ruoya, L. Xiang, Filtration characteristics of garnet media before and after modification, J. Water Reuse Desalin. 10 (2020) 133–145, https://doi.org/10.2166/wrd.2020.070.
[104] J. Wang, Y. Wu, Y. Cao, G. Li, Y. Liao, Influence of surface roughness on contact angle hysteresis and spreading work, Colloid Polym. Sci. 298 (2020) 1107–1112, https://doi.org/10.1007/s00396-020-04680-x.
[105] S. Minowa, H. Maeda, Preparation of hydrogarnet/poly(lactic acid) composite adsorbents for humic substance removal, Materials (Basel) 16 (2022) 336, https://doi.org/10.3390/ma16010336.
[106] T. Wajima, Conversion of blast furnace slag into hydrogarnet for humic acid removaL, Int. J. Geomate 22 (2022), https://doi.org/10.21660/2022.89.gxi353.
[107] J. Zhou, Y. Xia, Y. Gong, W. Li, Z. Li, Efficient natural organic matter removal from water using nano-MgO coupled with microfiltration membrane separation, Sci. Total Environ. 711 (2020), 135120, https://doi.org/10.1016/j.scitotenv.2019.135120.
[108] K.L. Jarvis, P. Majewski, Plasma polymerized allylamine coated quartz particles for humic acid removal, J. Colloid Interface Sci. 380 (2012) 150–158, https://doi.org/10.1016/j.jcis.2012.05.002.
[109] K.L. Jarvis, P. Majewski, Influence of film stability and aging of plasma polymerized allylamine coated quartz particles on humic acid removal, ACS Appl. Mater. Interfaces 5 (2013) 7315–7322, https://doi.org/10.1021/am401648g.
[110] K.L. Jarvis, P. Majewski, Optimizing humic acid removal by modifying the surface chemistry of plasma polymerized allylamine coated particles, Plasma Process. Polym. 13 (2016) 802–813, https://doi.org/10.1002/ppap.201500205.
[111] G. Kyzas, M. Kostoglou, Green adsorbents for wastewaters: a critical review, Materials (Basel) 7 (2014) 333–364, https://doi.org/10.3390/ma7010333.
[112] H. Soleimani, A.H. Mahvi, K. Yaghmaeian, A. Abbasnia, K. Sharafi, M. Alimohammadi, M. Zamanzadeh, Effect of modification by five different acids on pumice stone as natural and low-cost adsorbent for removal of humic acid from aqueous solutions - application of response surface methodology, J. Mol. Liq. 290 (2019), 111181, https://doi.org/10.1016/j.molliq.2019.111181.
[113] A. Zhang, W. Chen, Z. Gu, Q. Li, G. Shi, Mechanism of adsorption of humic acid by modified aged refuse, RSC Adv. 8 (2018) 33642–33651, https://doi.org/10.1039/C8RA05933K.
[114] M.A. Zulfikar, E. Novita, R. Hertadi, S.D. Djajanti, Removal of humic acid from peat water using untreated powdered eggshell as a low cost adsorbent, Int. J. Environ. Sci. Technol. 10 (2013) 1357–1366, https://doi.org/10.1007/s13762-013-0204-5.
[115] A. Mehri, G. Kashi, S. Khoramneghadian, N. Nourieh, Investigating the efficiency of humic acid removal from aquatic solutions with eggshell adsorbent, Desalin. Water Treat. 266 (2022) 247–255, https://doi.org/10.5004/dwt.2022.28613.
[116] H. Albatrni, H. Qiblawey, M.J. Al-Marri, Walnut shell based adsorbents: a review study on preparation, mechanism, and application, J. Water Process Eng. 45 (2022), 102527, https://doi.org/10.1016/j.jwpe.2021.102527.
[117] R. Yousef, H. Qiblawey, M.H. El-Naas, Adsorption as a process for produced water treatment: a review 8 (2020), https://doi.org/10.3390/pr8121657.
[118] I. Langmuir, The constitution and fundamental properties of solids and liquids. Part I. Solids, J. Am. Chem. Soc. 38 (1916), https://doi.org/10.1021/ja02268a002.
[119] H. Albatrni, H. Qiblawey, M.H. El-Naas, Comparative study between adsorption and membrane technologies for the removal of mercury, Sep. Purif. Technol. 257 (2021), 117833, https://doi.org/10.1016/j.seppur.2020.117833.
[120] R. Black, M. Sartaj, A. Mohammadian, H.A.M. Qiblawey, Biosorption of pb and cu using fixed and suspended bacteria, J. Environ. Chem. Eng. 2 (2014) 1663–1671, https://doi.org/10.1016/j.jece.2014.05.023.
[121] N. Ayawei, A.N. Ebelegi, D. Wankasi, Modelling and interpretation of adsorption isotherms, J. Chem. 2017 (2017) 1–11, https://doi.org/10.1155/2017/3039817.
[122] H.M. Freundlich, Over the adsorption in solution, J. Phys. Chem. 57 (1906) 1100–1107.
[123] H. Albatrni, H. Qiblawey, F. Almomani, S. Adham, M. Khraisheh, Polymeric adsorbents for oil removal from water, Chemosphere 233 (2019), https://doi.org/10.1016/j.chemosphere.2019.05.263.
[124] S. Lagergren, About the theory of so-called adsorption of soluble substances, K. Sven. Vetenskapsakademiens Handl. 24 (1898) 1–39.
[125] Y. Ho, G. McKay, Pseudo-second order model for sorption processes, Process Biochem. 34 (1999) 451–465, https://doi.org/10.1016/S0032-9592(98)00112-5.
[126] M.A. Al-Ghouti, J. Sayma, N. Munira, D. Mohamed, D.A. Da'na, H. Qiblawey, A. Alkhouzaam, Effective removal of phenol from wastewater using a hybrid process of graphene oxide adsorption and UV-irradiation, Environ. Technol. Innov. 27 (2022), 102525, https://doi.org/10.1016/j.eti.2022.102525.
[127] K.L. Tan, B.H. Hameed, Insight into the adsorption kinetics models for the removal of contaminants from aqueous solutions, J. Taiwan Inst. Chem. Eng. 74 (2017) 25–48, https://doi.org/10.1016/j.jtice.2017.01.024.
[128] S.-H. Yoon, C.-H. Lee, K.-J. Kim, A.G. Fane, Effect of calcium ion on the fouling of nanofilter by humic acid in drinking water production, Water Res. 32 (1998) 2180–2186, https://doi.org/10.1016/S0043-1354(97)00416-8.
[129] N. Fatima, A. Jamal, Z. Huang, R. Liaquat, B. Ahmad, R. Haider, M.I. Ali, T. Shoukat, Z.A. ALOthman, M. Ouladsmane, T. Ali, S. Ali, N. Akhtar, M. Sillanpää, Extraction and chemical characterization of humic acid from nitric acid treated lignite and bituminous coal samples, Sustainability 13 (2021) 8969, https://doi.org/10.3390/su13168969.
[130] Y. Yustiawati, K. Kihara, H. Sazawa, M. Kuramitz, T. Kurasaki, T. Saito, M. S. Hosokawa, L.Wulandari Syawal, I. Hendri, S. Tanaka, Effects of peat fires on the characteristics of humic acid extracted from peat soil in Central Kalimantan, Indonesia, Environ. Sci. Pollut. Res. 22 (2015) 2384–2395, https://doi.org/10.1007/s11356-014-2929-1.
[131] S. Yan, N. Zhang, J. Li, Y. Wang, Y. Liu, M. Cao, Q. Yan, Characterization of humic acids from original coal and its oxidization production, Sci. Rep. 11 (2021) 15381, https://doi.org/10.1038/s41598-021-94949-0.
[132] Y. Dergham, What are Humic Acids and Their Sources?, 2014.